Oil & Energy

HYDRO

Peon Discovery Report PL 318

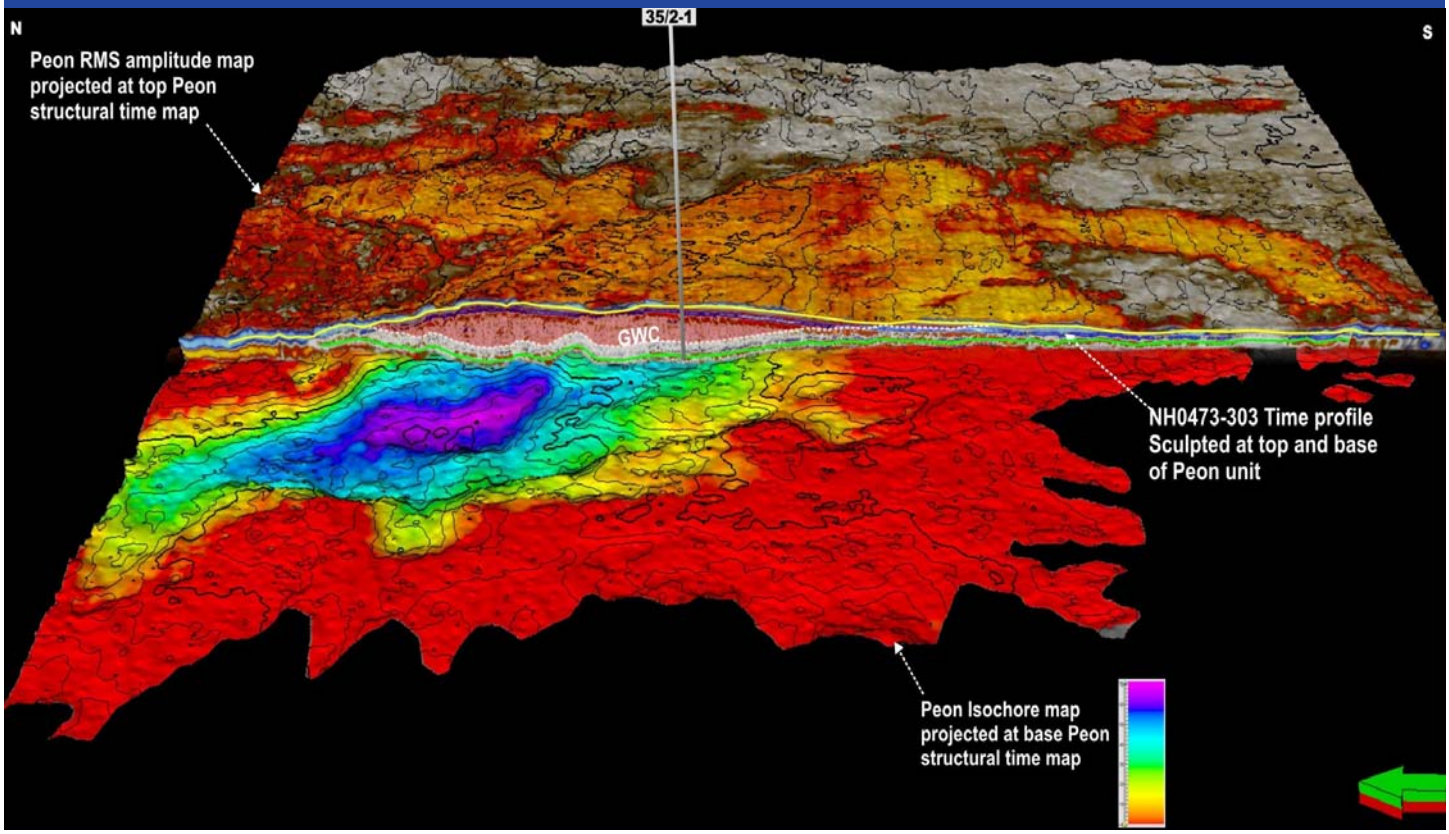

February 2006

出光 IDEMITSU

petoro

Oil & Energy
Development Norway

HYDRO

REPORT

Author(s): Espen Sletten Andersen, Trude Kristing, Dag Mustad, Anja Irene Relbo, Terje Solli

Report no.: NH-01201242
Date: 2006-03-03
Page: 1 of 69
Verified by: Bjørn Inge Braathen
Verified by: Terje Solli
Approved by: Odd Ragnar Heum

Peon Discovery Report

Summary:

The Peon dry gas discovery was made in July-August 2005 in PL 318 by exploration well 35/2-1. The reservoir is the shallowest reservoir targeted by exploration drilling in the Norwegian sector of the North Sea so far, with a top reservoir depth of 540 m MSL. The Peon structure is a rather massive sand body with a large area. The water depth is 380 m, giving an overburden ("seal") of only 160 m at well location. The reservoir is Middle Pleistocene, glacial deposited sands of the Naust Formation. The glasio-marine mound is interpreted to be a single reservoir, with no compartments due to faults or lithostratigraphic segmentation. The discovery well penetrated 9 m below the apex of the sand body. The GWC in the well is clearly defined on logs at 568 m MSL, with a saturation of 87% gas above the contact and 12-15 % below. The seismic velocity contrast between the gas zone and the water zone is hence low (near 860 m/s in logged values in both zones). This is considered a main reason for the lack of recognition of the GWC on seismic lines prior to drilling. Below the low saturated gas zone, the P-velocity jumps to 1800 m/s where there is pure brine sand, giving a good contrast on seismic lines. Methane of biogenic origin is the dominating component of the gas (99.14 Wt%). Two samples for PVT analyses were obtained in the well. The pressure gradients in the discovery well show 0.046 g/cc (0.0045 bar/m) in the gas zone and 1.019 g/cc (0.0999 bar/m) in the water zone. The gas gradient is confirmed by PVT analysis of gas samples from MDT. No cores were attempted cut in the loose sand. Attempts to recover sidewall cores were not successful, therefore no direct measurements of reservoir data are available. Based on log data, the average porosity in the gas zone is 36.0%, the net to gross is 98.7%. The expected GIIP for the Peon discovery is 36 GSm^3. The discovery well has been temporarily abandoned. It will be re-entered and a production test (DST) will be carried out, probably during 2nd or 3rd Quarter 2006. The present development scenario for Peon includes 5 vertical production wells tied back to a semi-submersible production unit through a field production-loop. Export can be provided through a 40 km pipeline to the Langeled-North dry gas export pipeline, where hot tapping is assumed directly into the pipeline. The productivity of the wells is expected to be high, with an average rate of 2 MSm^3/d rate from each well.

Key words:

Peon, dry gas, gas discovery, methane, biogenic origin, PL 318, Sogn Graben, Naust Fm, Pleistocene, glacial deposits, loose sand, Langeled

Distribution list:

PL 318 partners, NPD, MPE

CONTENTS

FIGURE LIST

HYDRO

TABLE LIST

1 INTRODUCTION

This report gives a summary of the present state of evaluation of the Peon gas discovery. It represents the end of the exploration phase of the Peon discovery and marks the hand over from the Exploration Department to the Field Development within Norsk Hydro. It has been concluded that the Peon discovery has a commercial potential and field development studies (Feasibility studies) will now be initiated.

The Peon dry gas discovery was made by exploration well 35/2-1, drilled in July-August 2005.

Norsk Hydro, as Operator of the PL 318 licence, drilled the well. The licence partners group in PL 318 are:

Norsk Hydro Produksjon AS	60%
Idemitsu Petroleum Norge AS	20%
Petoro AS	20%

The discovery was made in glacial sand deposits of Middle Pleistocene age. The Peon reservoir is very shallow, with apex depth at 540 m MSL and gas water contact at 568 m MSL. The Peon sand reservoir is a massive body, consisting of two main coarsening upwards units. The sands are of extremely good reservoir quality, with average porosity of 33.2%. During drilling it proved impossible to obtain side-wall core samples in the loose sand interval, therefore no direct permeability data have been obtained.

The resource estimate (GOIP) in the Peon gas discovery is

Gas Originally in place (GSm^3)		
P90	Expected	P10
31.0	36.0	41.1

2 DATA BASE

2.1 Well Data

The well data (formation evaluation data) acquisition programme of the reservoir interval includes sidewall cores, LWD logs and Wire Line logs (e.g. FMI log, MDT Formation pressure data, MDT Fluid samples, and PVT Data).

2.2 Seismic Data Base and data quality

The entire licence area is covered by 2D and 3D seismic data (**Figure 2-1** and **Figure 2-2**). The full-fold version of the merged MS97M 3D seismic survey was the primary data set used for evaluating the area.

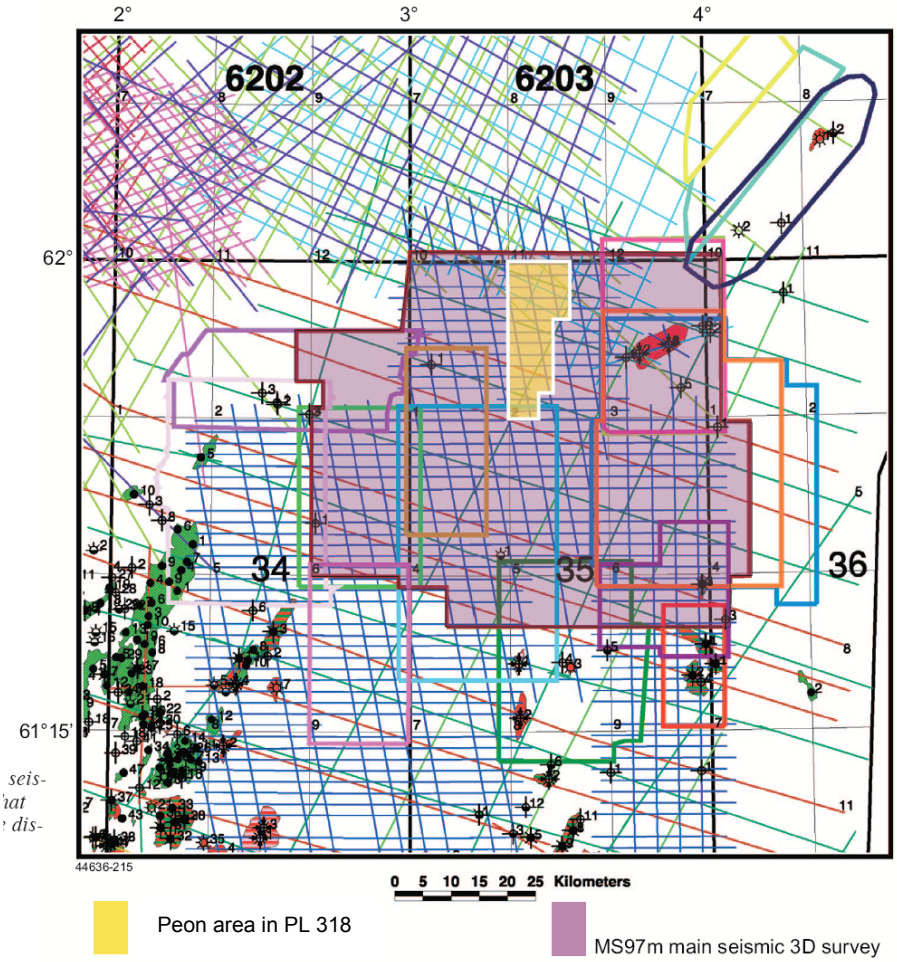

Figure 2-1. Well and seismic database. Note that not all 2D surveys are displayed.

The full fold version of MS97M is the main survey used in the seismic interpretation. Neighbouring seismic surveys, especially, NH03M3 and ST98M8, were important when evaluating the Quaternary sand deposits in the province. Several 2D seismic surveys have been used in order to delineate the Peon prospect to the north.

The well prognosis, as well as the drilling-/geo-hazard assessment, was performed using high-resolution 2D seismic data (NH0473). The seismic lines form a 250x250m and 500x500m grid covering the eastern part of the Peon discovery (**Figure 2-2**). The high-resolution 2D seismic is of good quality resolving every important event in the shallow section (i.e. between seabed and Top Peon; **Figure 2-3**).

The 3D seismic surveys are generally of good quality, but the seismic character varies considerably in the shallow section (**Figure 2-3**).

Table 2-1. Geophysical database

Survey	Company	Contractor	Vintage
BPN9401M00	BP		1994 / 2000
MC3D-Q34	NOPEC	PGS / GGG	1995 / 1997
MS97M	Hydro	PGS	1997 / 1998
NH9402_FINAL	HYDRO	PGS / CGG	1994 / 2000
NH03M3	Hydro	CGG	2005
NVG 2000	GEOTEAM	GEOTEAM	2000
ST98M8	Statoil	CGG	1999
GP3D93	NEPS/Total	GECO-PRAKLA	1993/1994
GMNR94 (2D)	WesternGeco	WesternGeco	1994
NH0473 (2D)	Hydro	Fugro Survey	2004
2D surveys: NVGTI-92, MS99, NVGT88, NOD4-84, GMS1-91, GMS-85, MS-85 & MSI-99			

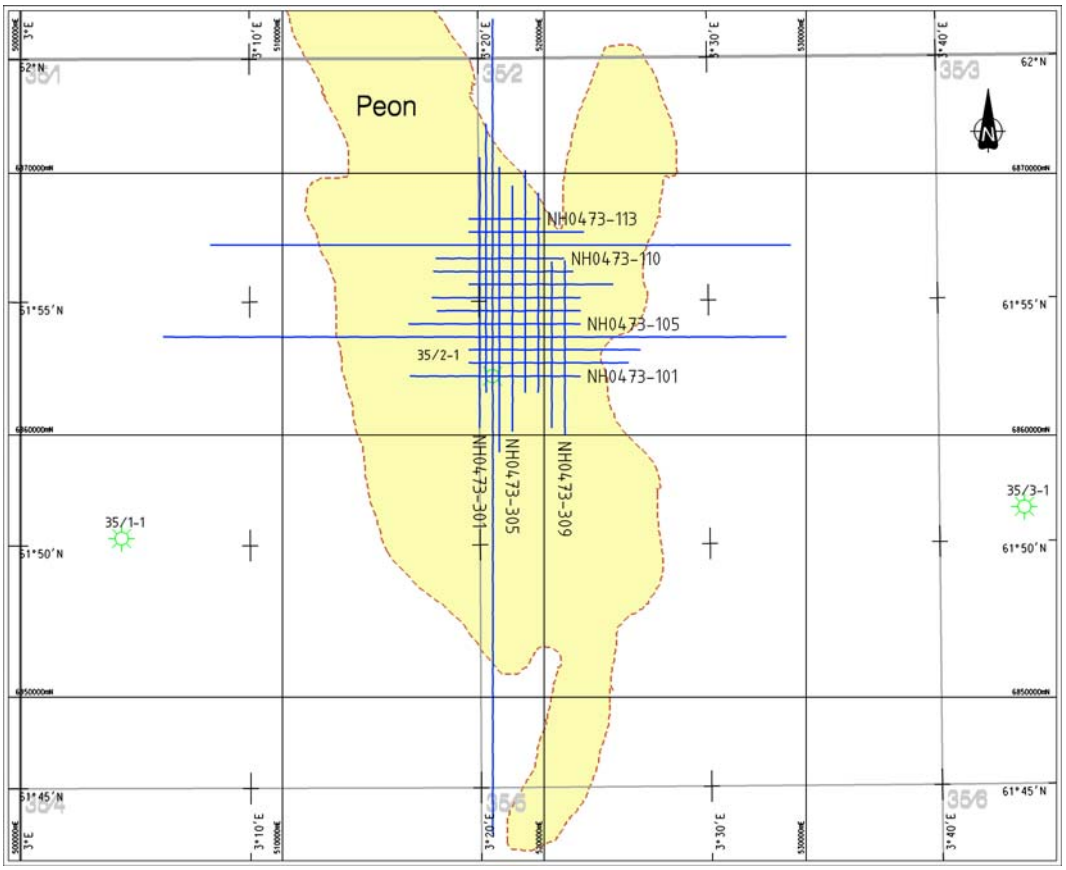

Figure 2-2. NH0473 High-resolution 2D survey grid.

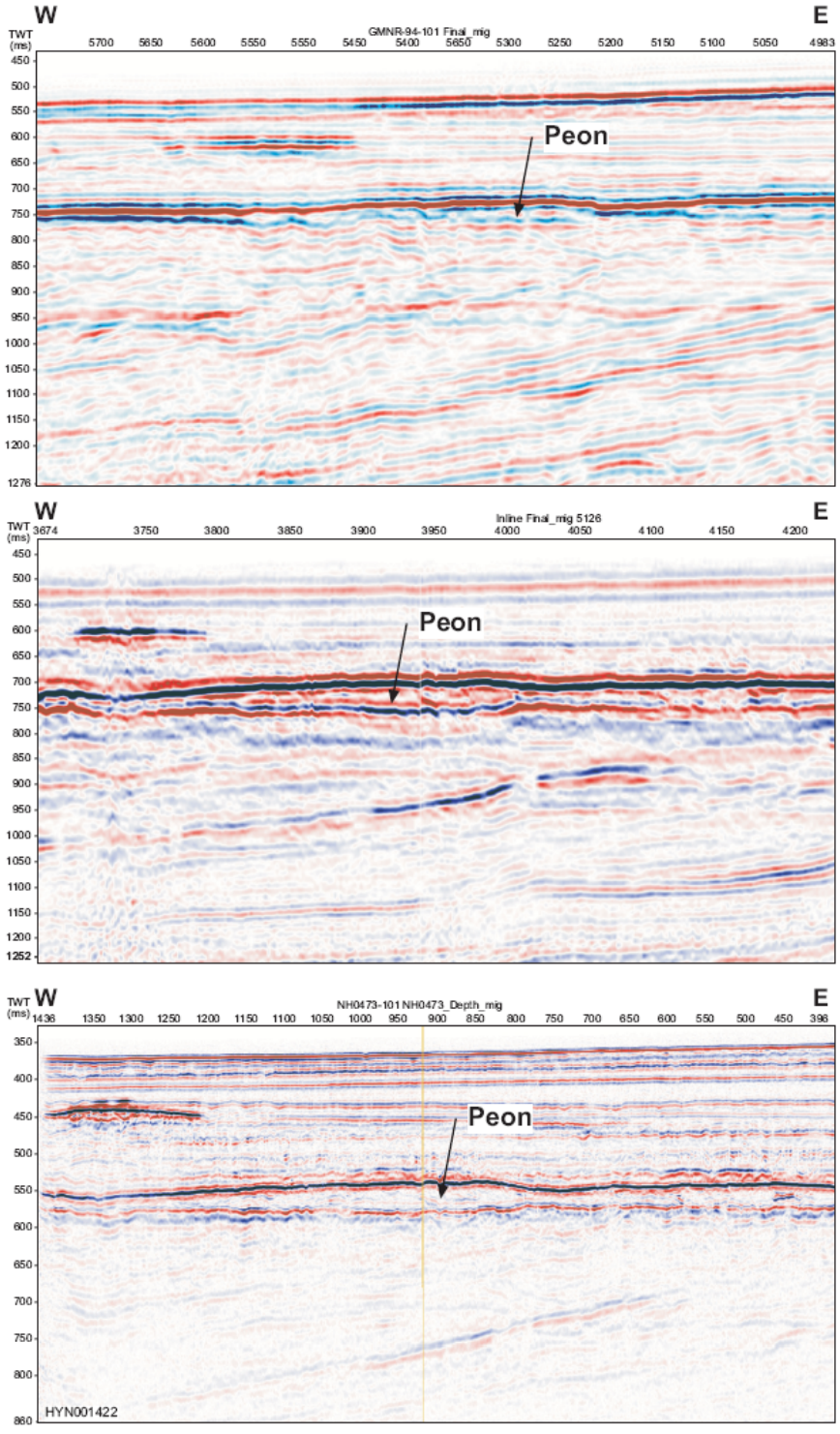

Figure 2-3. Three seismic sections crossing Well 35/2-1, exhibiting large difference in seismic resolution and quality. Upper panel: Regional exploration 2D data, GMNR94; Middle panel: Good quality exploration 3D data, MS97M; Lower panel: High-resolution 2D PSDM data, NH0473.

3 GEOPHYSICAL EVALUATION

3.1 Prospect mapping and history

3.1.1 Mapping and Depositional Environments

The spectacular Peon anomaly was discovered by IKU in the early nineteen eighties as part of their regional Quaternary Mapping Programme (IKU 1984), however the commercial possibilities were not obvious until 2000 when Hydro started working on the regional MS97M 3D dataset.

The Jurassic succession was the primary exploration target but the thorough investigation resulted in the discovery of the Quaternary Peon Prospect. Peon is *de facto* a shallow gas feature, however the following three key features transformed it into Hydro's first shallow gas discovery:

1. Structural four-way closure
2. Mounded morphology with a large volume potential
3. Distinct velocity push-down and AVO anomaly (AVO class III and IV)

The Peon Prospect Model was defined based on its relationship with a regional angular unconformity, an important boundary formed by glacier ice, separating steeply dipping Pliocene strata from sub-horizontal strata of Pleistocene age. As the seismic data indicates that Peon was deposited above the unconformity (being younger), strongly suggests that it was deposited in a glacial or glacial-marine environment, probably as a drumlin (sub-glacial) or as an outwash delta ridge (in front of a former glacier).

The fact that the Peon mound has been preserved, in spite of following ice advances crossing the site, is a key observation in order to evaluate its reservoir properties. The fact that the positive feature is preserved clearly suggests that Peon consists of sediments with high porosity and permeability (i.e. sand and gravel) as sub-glacial deposition/non-erosion occurs where water can drain from the bed. On the other hand, if water pore-pressure is high (e.g. clay-rich sediments beneath an ice stream) sub-sole deformation is promoted and any protruding feature will be levelled out.

The Peon prospect was therefore regarded as a huge sand depo-centre prior to drilling. Enormous quantities of well-sorted Eocene-to-Oligocene sands were available, outcropping 15-30 kilometres to the east and southeast at the time of deposition, and most likely transported by sub-glacial water and deposited in front of the glacier.

3.1.2 Seismic Data Analyses

The various geophysical observations prior to drilling suggested a high probability for Peon being a gas-filled sand with good reservoir properties:

"Bright Spot": - The prospect is characterized by a distinct seismic amplitude anomaly and well-defined phase-reversals towards east and west (**Figure 3-1**).

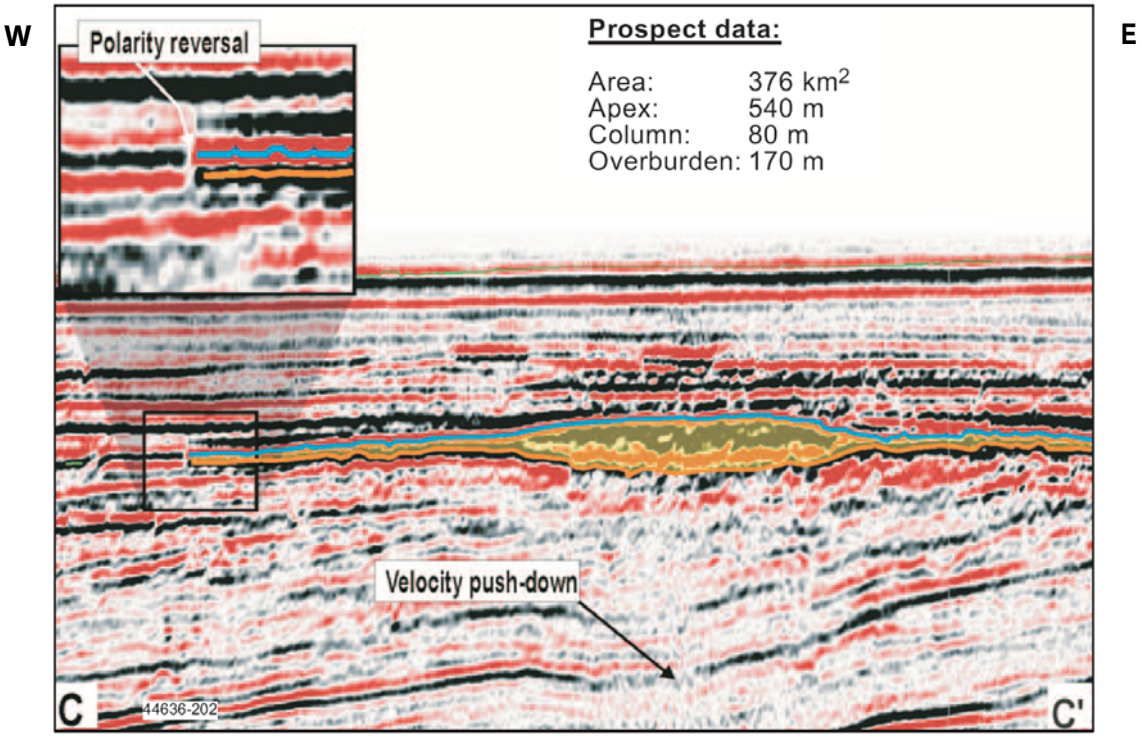

Figure 3-1. The Peon prospect shows every sign of shallow gas: Anomalously high amplitude, phase reversed reflections (bright spot), allied to a number of other characteristics, such as acoustic masking within and below, velocity push-down, structural closure, frequency reduction. No basal flat spot is observed, which prior to drilling was explained as a down-to situation (i.e. the prospect was completely filled with gas).

Class IV AVO anomaly: - The pre-stack analyses show a distinct AVO class IV anomaly at top and base of the reservoir interval. The seismic anomaly defining the prospect reflects a low acoustic impedance, low Vp/Vs and low acoustic velocity (Vp) body, typical for gas-bearing sediments.

High porosity and high gas saturation: - A manual inversion study performed by Hydro in order to estimate the densities within the prospect showed that the estimated Peon densities are typically significantly lower than the 1.80 g/cc expected for 36% porosity and 80% gas saturation. The surprising results suggest that the calculations are based on incorrect assumptions and that significant changes must be made to the assumptions in order to produce realistic density estimates. Thus, to the best of our knowledge, the Peon anomaly appears to be consistent with high porosity and high gas saturation.

Velocity effects: - Velocity pushdown-effects and frequency-reduction are observed below the prospect and acoustic masking within the thicker part of the prospect are convincing evidences for the presence of gas.

Lack of "flat spot": - In the pre-drilled prospect model the whole reservoir body within the amplitude anomaly was completely filled with gas, explaining the lack of flat spot.

3.1.3 Volume and Risk

The shallower part of the prospect has a four-way dip closure with a column of approximately 16 m, however a large gas volume trap was indicated depending on stratigraphic sealing to the south. The pre-drilled apex of the structure was estimated to 544 m (below MSL) with anticipated dry gas column of 82 m. The overburden consists of approximately 200 meters of predominantly glacially derived clay with high sealing potential. The main risk was related to gas saturation, effective top seal and reservoir characteristics.

All pre-drilling assumptions and conclusions were confirmed by the post-well studies, except for the gas column being 58 m less than anticipated. The difference in prospect outline is shown in **Figure 3-2**.

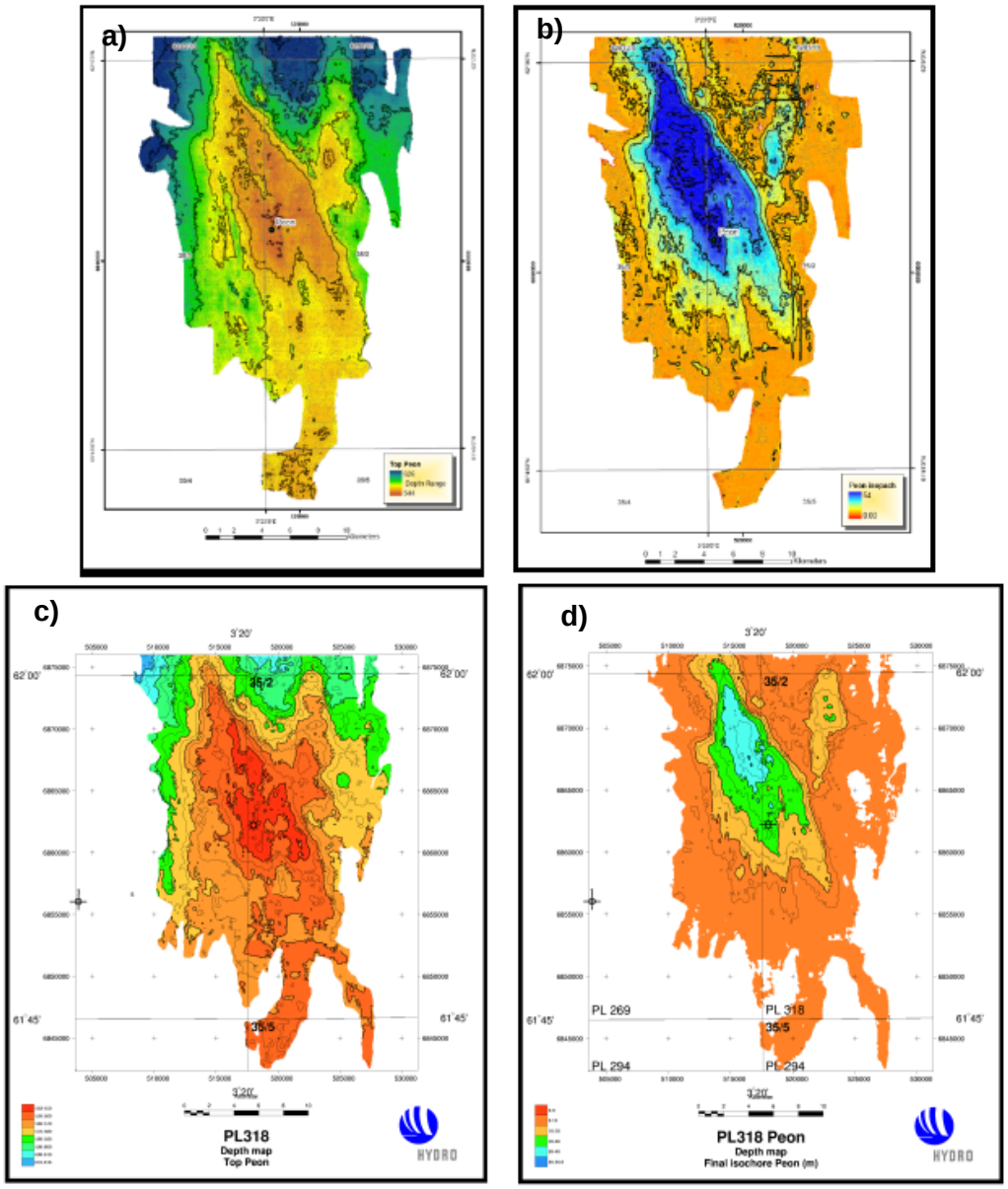

Figure 3-2. Depth structure and thickness maps. a) Structural map before drilling, b) Isochor map prior to drilling, c) Structural map after drilling d) Isochor map after drilling.

3.2 Well tie and AVO response

3.2.1 Seismic Prognosis compared with actual results

The pre-drill depth prognosis was reasonably good but with a consistent trend towards reflectors and contact being observed 0.5 to 13.5 m (increasing with depth) shallower than anticipated in the well area. This has been corrected by the post-drill depth conversion.

Structural apex was encountered as expected. The GWC at 568 m MSL was 58 m shallower than the anticipated spill, while top of the reservoir section came in 2 m shallower than anticipated.

In terms of seismic interpretation, most reflectors in the Quaternary succession occurred as anticipated (i.e. within the uncertainty bracket), and with the same approximate vertical separations as suggested before drilling. R116 (intra-Pliocene?) was outside the prognosis, appearing 13,5 m shallower than expected. The relatively large error is most likely caused by unexpectedly low reservoir velocity and the occurrence of a thin sand layer immediately below the main sand reservoir, also adding low velocities to the system.

Table 3-1. Pre-drill prognosis compared with actual results from Well 35/2-1.

	Expected	Actual
Phase	Gas	Gas
GOIP	53.5 GSm^3	36 GSm^3
Apex	544 m MSL	544 m MSL
Top res in well	551±6 m MSL	549 m MSL
GDT	588±7 m MSL	
GWC		568 m MSL
HC column in well	37 m	19 m

3.2.2 Synthetic seismogram and well tie

3D seismic exploration data are usually not suited for detailed analysis of shallow geological features, because of the typically large and variable near offset distances and low fold, and the sometimes reduced seismic resolution due to NMO-stretch. High-resolution 2D seismic (intended for site surveys) are designed for studying shallow features, and thus much better suited for seismic-to-well tie for the Peon discovery.

The quality of a seismic-to-well tie depends on the quality of both the seismic data and the well logs. A near offset seismic-to-well tie requires P-velocity and density logs, while additional S-velocity data are needed for far offset (AVO) ties.

All logs required for seismic-to-well ties are available for the Peon discovery well 35/2-1. **Figure 3-3** shows the P-velocity, S-velocity, density, computed P-impedance, computed Vp/Vs ratio and resistivity logs, as well as the estimated lithology and saturation logs.

The high and low gas saturation parts of the reservoir are clearly visible in the P-velocity log. There is no contrast in P-velocity across the GWC (i.e. free water level), with logged values close to 860m/s for both the high gas saturation zone (above the GWC) and the low gas saturation zone (below the GWC). The P-velocity jumps to around 1800m/s in the brine sand below the low gas saturation zone.

The logged S-velocities are around 500m/s for the entire sand unit, with a variation of about +/-40ms, with the expected slightly higher values in the high gas saturation zone (because of the density effect), but no contrast at the base of the low gas saturation zone.

The logged densities (the black density curve in **Figure 3-3**) are clearly influenced by fluid invasion during drilling; the expected large increase in density at the GWC is barely visible. The red density curve in **Figure 3-3** shows the results of Gassman fluid substitution back to the estimated *in-situ* properties, giving the expected significant increase in density at the GWC. A shallower increase in density in the middle of the high gas saturation zone is probably related to a change in porosity (and saturation as a second order effect), as there are no indications of significant changes in mineralogy though the reservoir (**see section 5.3**).

The P-velocity and fluid substituted density logs have been used for seismic-to-well tie to the near offset version of site survey line NH0473-101, and the initial zero phase peak polarity wavelet was extracted from the near offset seismic data. Two contrasts completely dominate the P-impedance log; the top of the reservoir and the base of the low gas saturation zone. The initial seismic tie is shown in **Figure 3-4**, after alignment of the top of the Peon reservoir. The red trace is the near offset seismic trace at the well location, and the blue trace is the synthetic response to contrasts in the P-impedance log. Note that the TWT thickness according to the logged P-velocities (~860m/s) does not match the seismic TWT thickness of the high and low gas saturation reservoir. The seismic TWT thickness suggests an average P-velocity of ~950m/s.

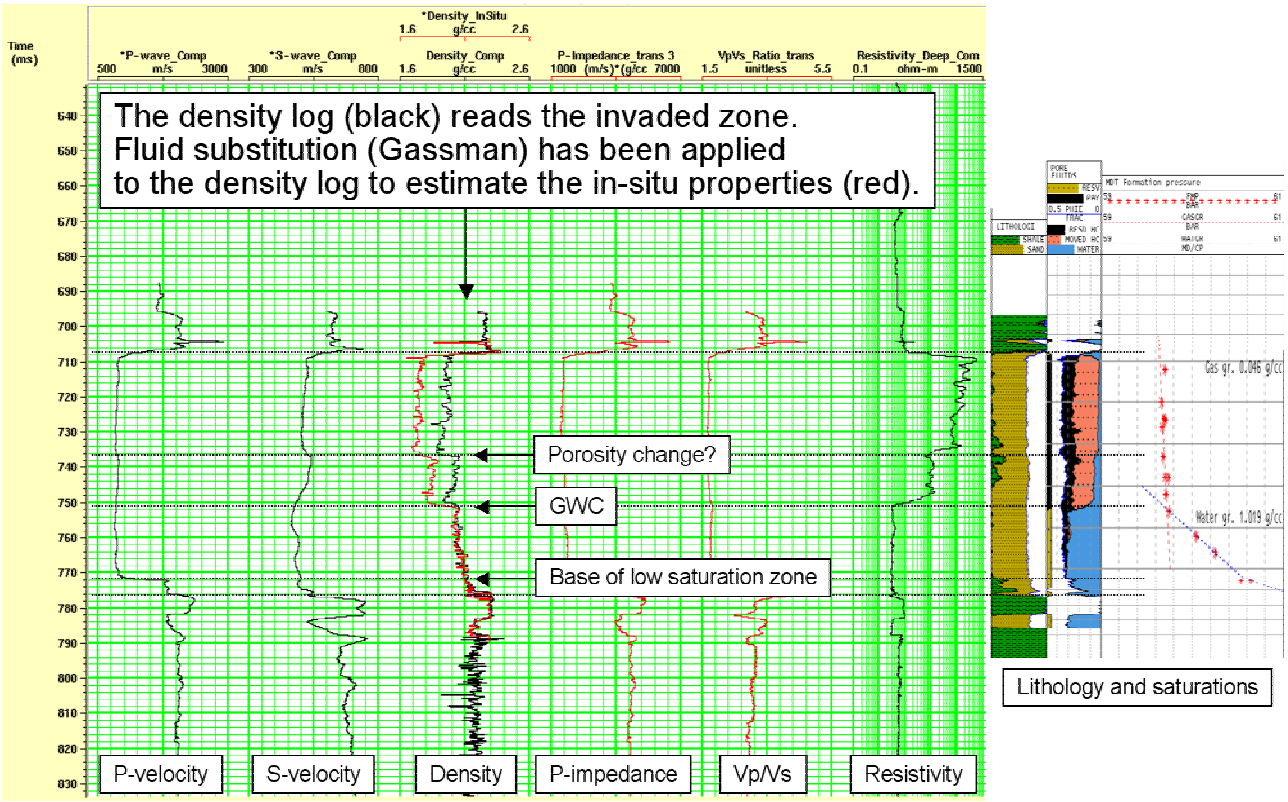

Figure 3-3. 35/2-1 well logs: P-velocity, S-velocity, density, computed P-impedance, computed Vp/Vs ratio and resistivity, as well as the estimated lithology and saturation logs. The red density curve shows the results of Gassman fluid substitution back to the estimated in-situ properties, giving the expected significant increase in density at the GWC.

Figure 3-5 displays the final seismic-to-well tie after alignments of the reflections from the top of the reservoir and the base of the low saturation zone. The updated P-velocity log is shown in red. A wavelet phase rotation of -40deg. produces a symmetrical synthetic-to-real cross-correlation function for the time window 720-800 ms, and thus the near offset data appear to be about -40deg. from zero phase peak polarity. (The reflection from the top of the reservoir has been excluded from the phase estimation exercise since it sits so close to the start of the logs. Including the top reflection gives a phase deviation of about -10deg.). Note that a weak positive reflection is expected for the GWC.

In **Figure 3-6** the P-impedance log is added to the near offset seismic section. A weak positive reflection coincides with the GWC at the well location. Where visible and continuous, this event appears to be parallel to the base reflection, and this is as expected for the GWC reflection since the P-velocity does not change across the GWC. The soft reflection from the top of the reservoir does not appear to be completely symmetrical, matching the phase prediction from the seismic-to-well tie.

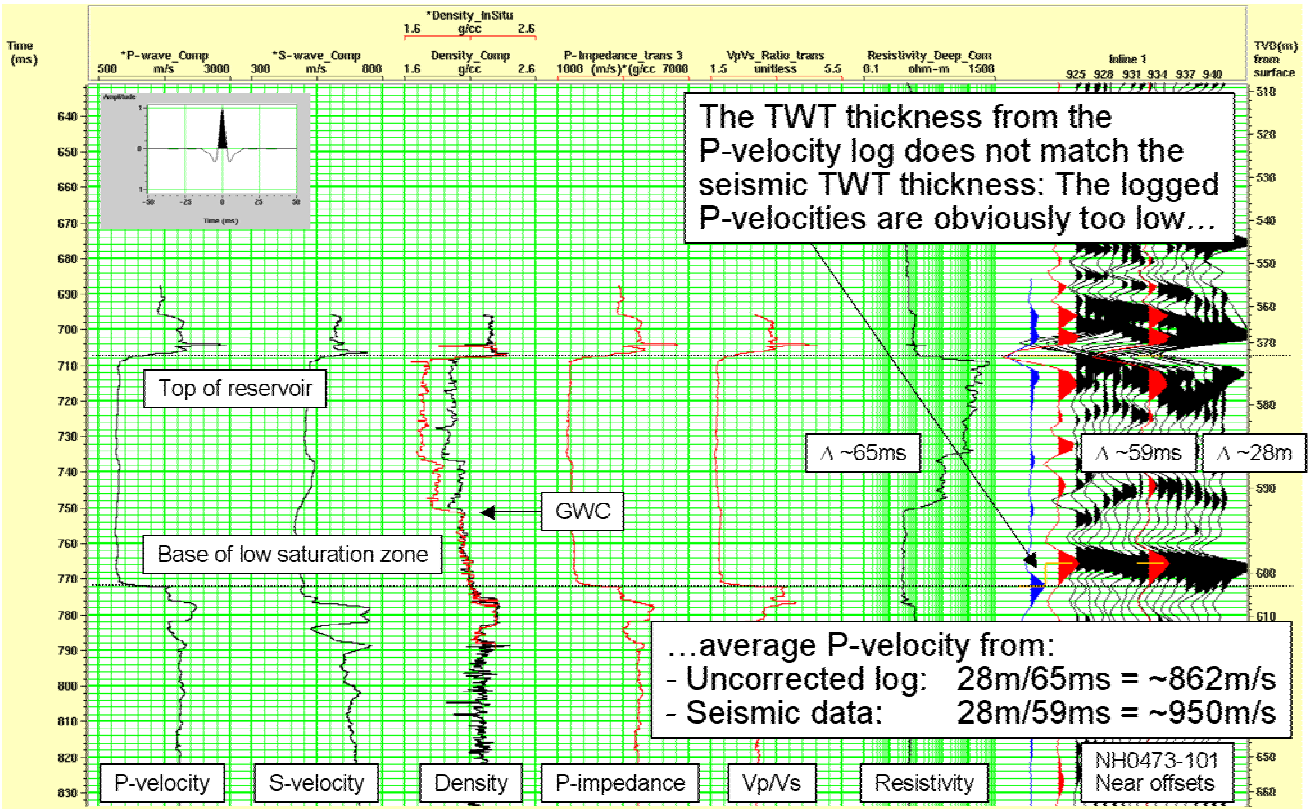

Figure 3-4. Initial NH0473-101 near offset seismic-to-well tie, after alignment of the top of the reservoir. Synthetic trace in blue, near offset seismic trace at the 35/2-1 well location in red. Zero phase peak polarity wavelet extracted from the data. Note the initial miss-tie for the reflection from the base of the Peon anomaly.

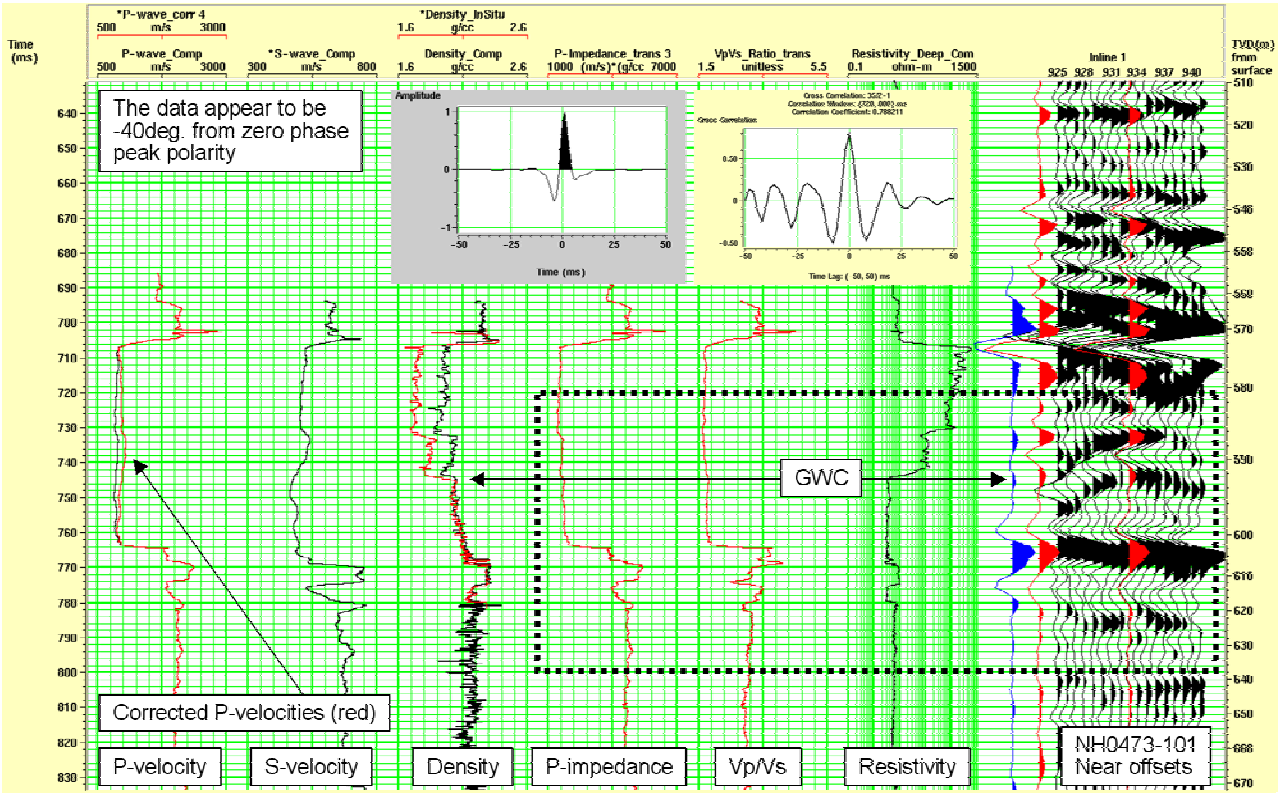

Figure 3-5. Final NH0473-101 near offset seismic-to-well tie. Updated P-velocity log in red. A wavelet phase rotation of -40deg. produces a symmetrical synthetic-to-real cross-correlation function for the time window 720-800ms. Note that a weak positive reflection is expected for the GWC.

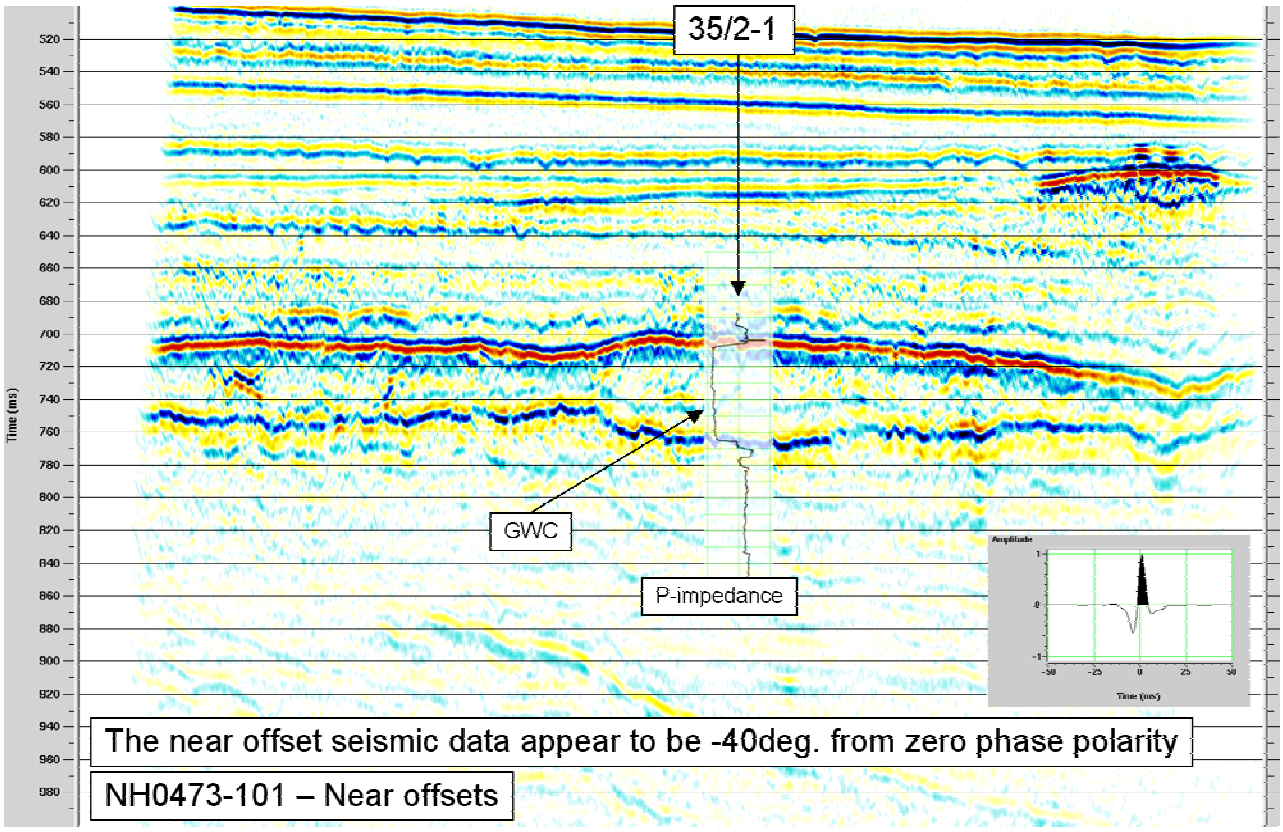

Figure 3-6. High-resolution survey NH0473-101 near offset seismic section. Red colours represent negative values. P-impedance log inserted at the 35/2-1 well location. A weak positive reflection coincides with the GWC at the well location. The soft reflection from the top of the reservoir does not appear to be completely symmetrical, matching the phase prediction from the seismic-to-well tie.

3.2.3 Expected AVO responses

The blocky appearance of the logs makes the transformation into a simplified model straightforward. The simple model in **Figure 3-7** matches the logged data very well. The low velocity reservoir interval is clearly visible. The average brine sand values fill the half space below the gas reservoir. The expected AVO responses based on this simple model are:

- Clay-to-(gas sand) (i.e. top reflection): Class 3 (& 4) AVO
- (Gas sand)-to-(brine sand) (i.e. base reflection): Weak Class (3 &) 4

Weak Class (3 &) 4 AVO is the typical combined top and base response from AVO cross-plotting of the NH0473 site survey data.

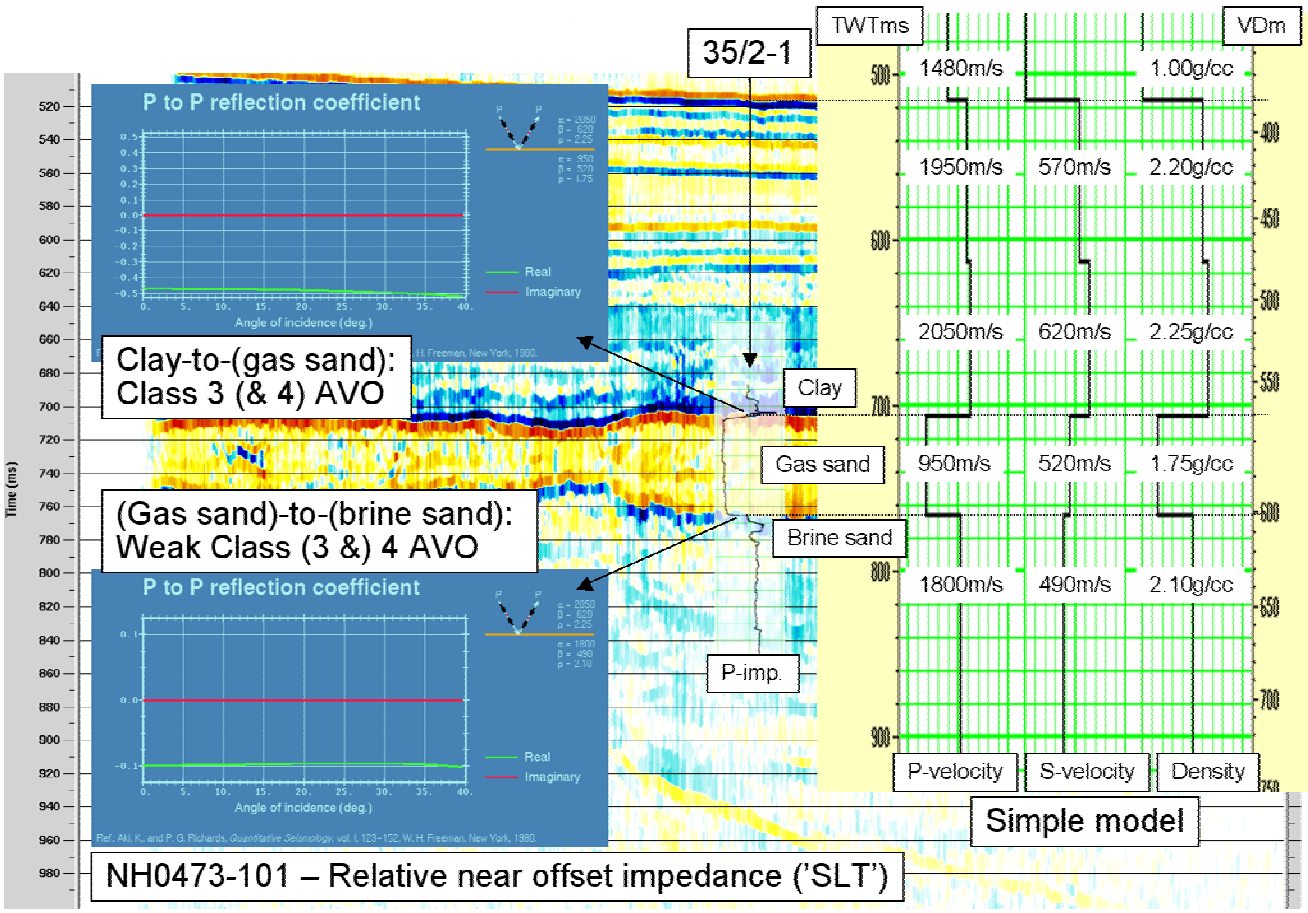

Figure 3-7. High-resolution survey NH0473-101 near offset relative impedance section. Red colours represent negative values. P-impedance log inserted at the 35/2-1 well location. Added are a simple AVO model matching the well logs (right) and the expected AVO responses for the clay-to-(gas sand) and (gas sand)-to-(brine sand) interfaces (left).

3.2.4 Seismic velocities

Using the observed pushdown effects in the seismic 3D data, the uncomfortably low initial interval P-velocity estimate was about 1275m/s (~ +/-65ms). Even lower estimates came from continuous velocity analysis of three site survey lines (and note the large standard deviations related to the extreme sensitivity to the accuracy of the top and base picks):

- NH0473-104: Average: 1168m/s (± 468 m/s) Median: 1115m/s
- NH0473-111: Average: 1244m/s (± 481 m/s) Median: 1249m/s
- NH0473-303: Average: 1195m/s (± 456 m/s) Median: 1194m/s

The corrected P-velocity log from well 35/2-1 gives an interval velocity of around 950m/s. This may seem anomalously low, but is in fact exactly what is predicted by a modified version of rock physics contact theory, in which the tangential stress (i.e. friction) between grains is set to zero. An interval P-velocity of 950m/s therefore appears to be the best estimate for the Peon reservoir.

In order to verify that Dix velocity inversion is able to resolve such low interval velocities, AVO modelling with subsequent velocity picking has been performed. The AVO modelling

result is shown in **Figure 3-8**, including the simple AVO model and the resulting gather with and without T^2 geometrical spreading correction. And according to the velocity picking result in **Figure 3-9**, Dix velocity inversion should be able to approximately resolve the very low interval velocity of around 950m/s. However, the interval velocity estimates from Dix formula for thin layers is very sensitive to the accuracy of the stacking velocity picks.

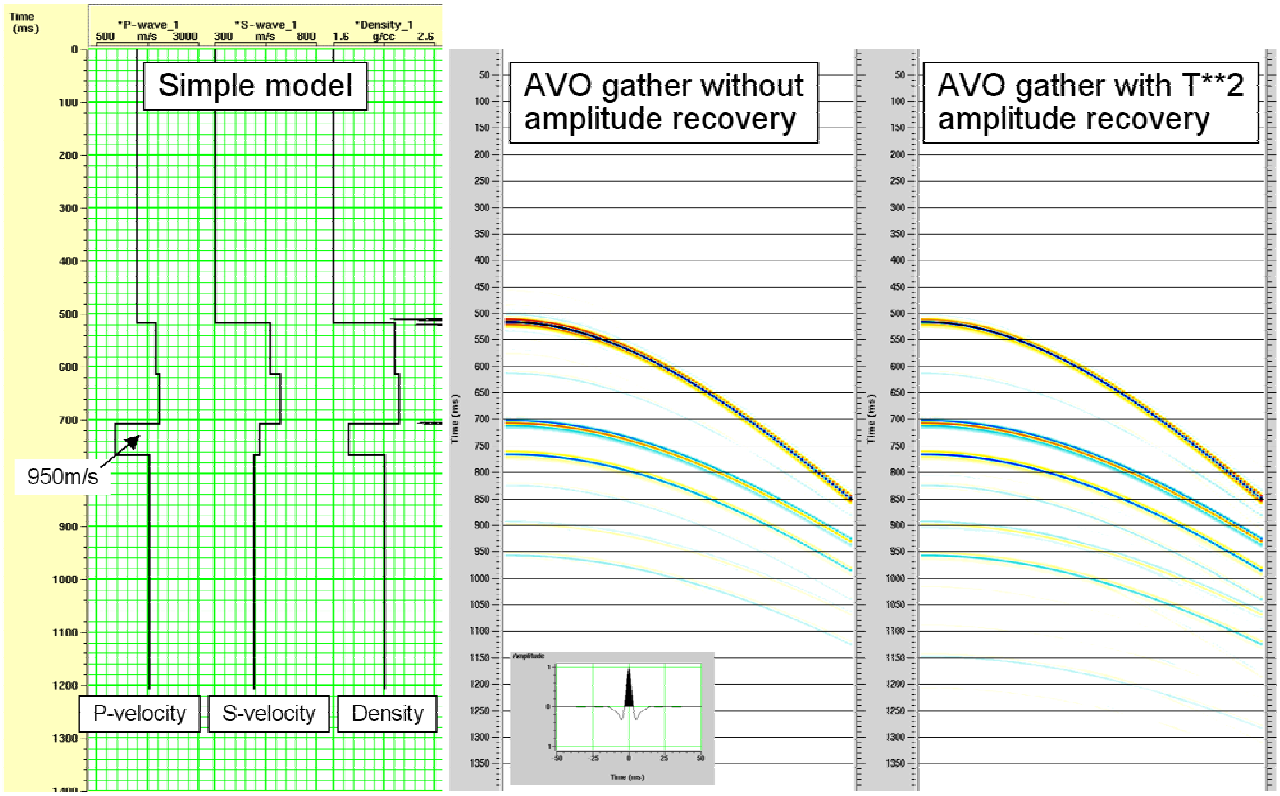

Figure 3-8. AVO modelling result for the simple AVO model from Figure 5, displayed with and without T^2 geometrical spreading correction. Modelling details: Full elastic AVO modelling ('Propagator matrix'), with all multiples and all wave conversions, and with transmission loss, geometrical spreading and absorption. Zero phase peak polarity wavelet from the seismic-to-well tie.

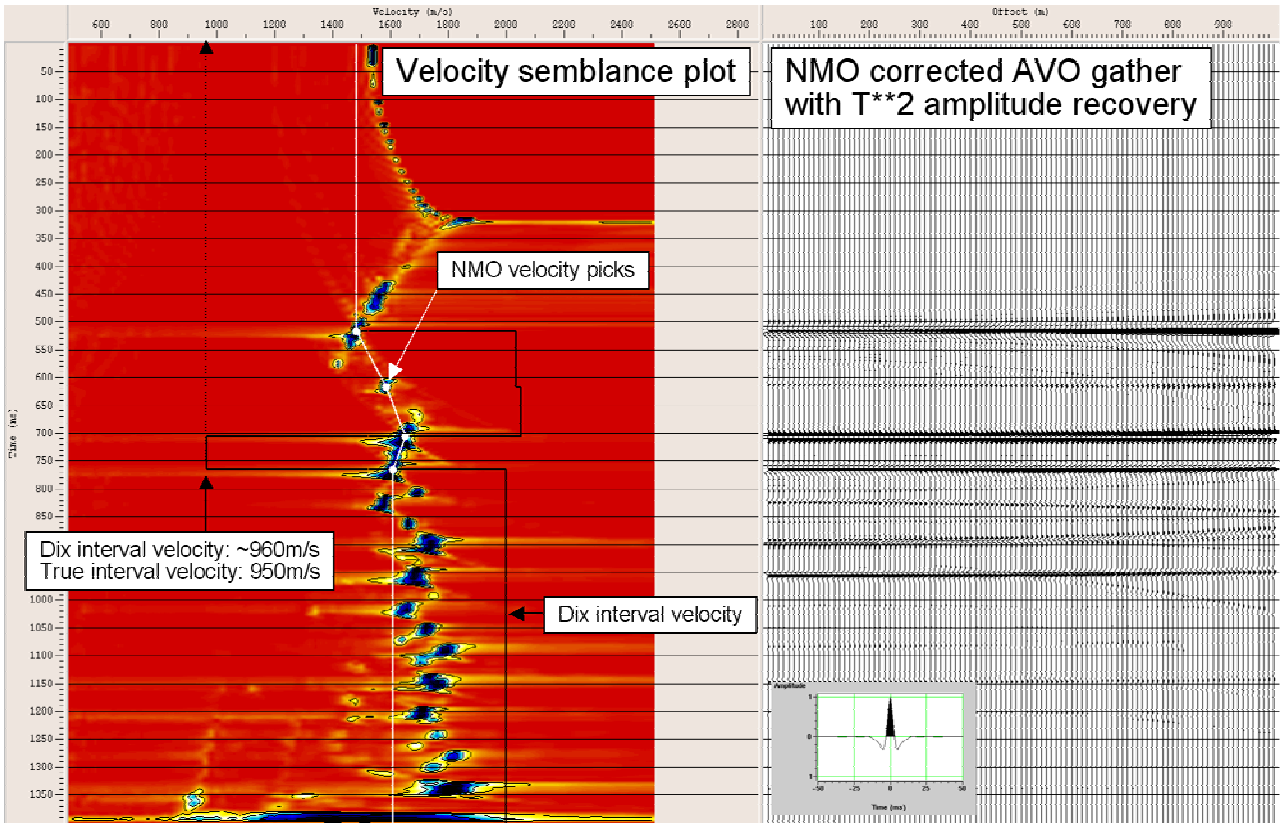

Figure 3-9. Stacking velocity picks for the AVO gather from Figure 6 (with T2 geometrical spreading correction). Dix velocity inversion is able to approximately resolve the very low interval velocity of around 950m/s.

3.3 Seismic interpretation

The seismic interpretation is based on the full-fold version of the MS97M 3D survey and some high-resolution 2D seismic sections from the NHH0473 survey (**Figure 3-10** and **Figure 3-11**).

Table 3-3 and **Figure 3-12** show the horizons interpreted on the NH0473 high-resolution 2D seismic dataset.

Table 3-2. Interpreted horizons using the MS97M 3D dataset.

MS97M –full fold 3D pre well	3.3.1.1 MS97M –full fold 3D post well
Sea bed	Top Peon
Upper Regional Unconformity	Base Peon
Intra Pliocene	Intra Lower Pleistocene Unconformity
Intra Miocene	
Intra Eocene	
Base Balder	
Top Lists fm	
Top Cretaceous	
Intra Maastrichtian	
Base Blodøks fm	
Intra Albian	
Base Cretaceous Unconformity	

Table 3-3. Picked horizons using the NH0473 high-resolution dataset.

Reflection	Description
R00 (Seabed)	Continuous and smooth, dipping to the west.
R10	Continuous with minor irregularities. Scattered elongated depressions are revealed on 3D time slices.
R20	Continuous with minor irregularities, dips gently to the WSW. Scattered elongated depressions are revealed on 3D time slices.
R30	Continuous and smooth, dipping WNW. Widespread uniform lineation revealed on 3D time slices (SSE-NNW).
R40	Continuous, smooth and almost horizontal. Scattered elongated depressions are revealed on 3D time slices.
R50	Continuous, smooth and almost horizontal. Anomalies show phase reversal. Widespread uniform lineation revealed on 3D time slices (SSE-NNW).
R55	Continuous, mark the top of an elongated, narrow ridge oriented SSE-NNW. Anomalies at top and apex show phase reversal.
R60	Continuous and smooth, dipping WNW. Merge with R50 approximately 5km west of Peon (Unit IX). Anomalies form an elongated sheet directly above R60.
R70	Continuous, irregular and almost horizontal. Scattered elongated depressions revealed on 3D time slices.
R80	Generally continuous, irregular (generating diffraction hyperbolas), and nearly horizontal. Scattered elongated depressions are revealed on 3D time slices.

Reflection	Description
R90 (Top Peon; Unit IX)	Top of mound shaped Peon deposit. Continuous and smooth (scattered diffraction hyperbolas). Scattered elongated depressions are revealed on 3D time slices.
Reflections within Peon (Unit IX)	Numerous Reflection fragments; low to very high amplitudes. Few continuous reflections; generally irregular, low to high amplitudes. Locally series of dipping reflections; in a north-south elongated area immediately west of Location, dips NNE and show medium amplitudes (Figure 4.7).
R100 (base of gas filled Peon sand)	Base of the gas filled Peon deposit. R100 is only revealed on the 2D data and occurs near base of Unit IX (Figure 4.8). At Location R100 coincide with the unconformity below, marked by reflection R101. These two reflections are not separated on the 3D data. R100 is irregular and dips gently to the northwest.
R101 (URU, Top Pliocene)	The reflection defines a regional angular unconformity (URU) truncating the northwest dipping beds below. R101 shows reversed polarity in areas where the Pleistocene deposits overlay Pliocene-to-Miocene deposits or Oligocene deposits. Dips gently to the northwest.
R110	Continuous, dipping approximately 5° to NW. Truncated by URU 1.9km NW of Location. Anomalies at truncation.
R111	Continuous, dipping slightly to NW. Truncated by URU 3km NW of Location.
R115	Continuous, dipping approximately 5° to NW. Truncated by URU 1.5km NW of Location.
R116	Continuous, dipping approximately 5° to NW. Truncated by URU 900m SE of Location.
R117	Continuous, dipping approximately 5° to NW. Truncated by URU 3.5km SE of Location. The anomalies are elongated in the fall direction.
R119	Occur in the SW part of survey area. It distinguishes an interval of high amplitude, parallel reflections below from a poorly stratified interval above.
R150 (Base Naust?, Top Miocene/ Pliocene)	Continuous, dipping NW. Anomalous in western part of area. Below R150: Sub-parallel, low to high amplitude reflections in the central and eastern part of the area, undulating and anomalous to the west. Above R150: high amplitude reflections down-laps onto R150 east of Location, sub-parallel, low amplitude reflections to the west.

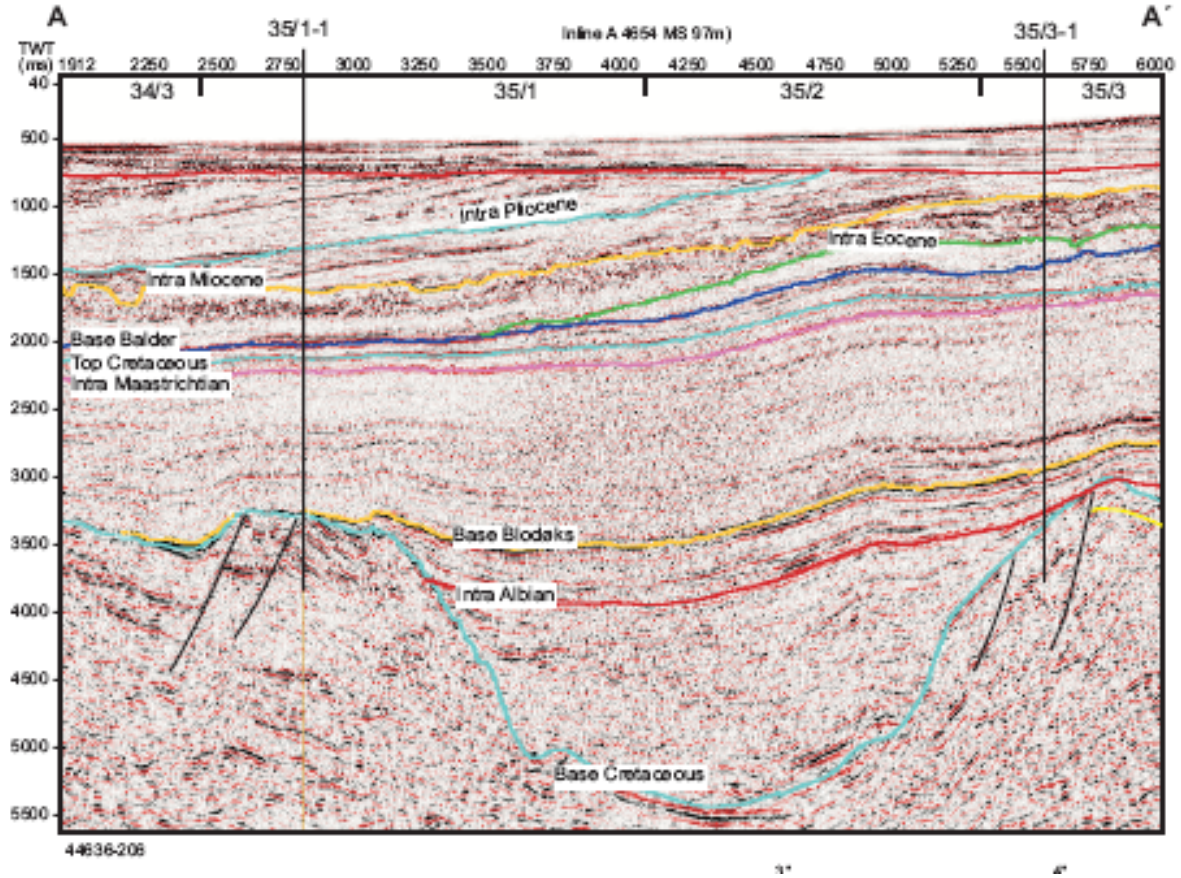

Figure 3-10 East West line across Sogn Graben.

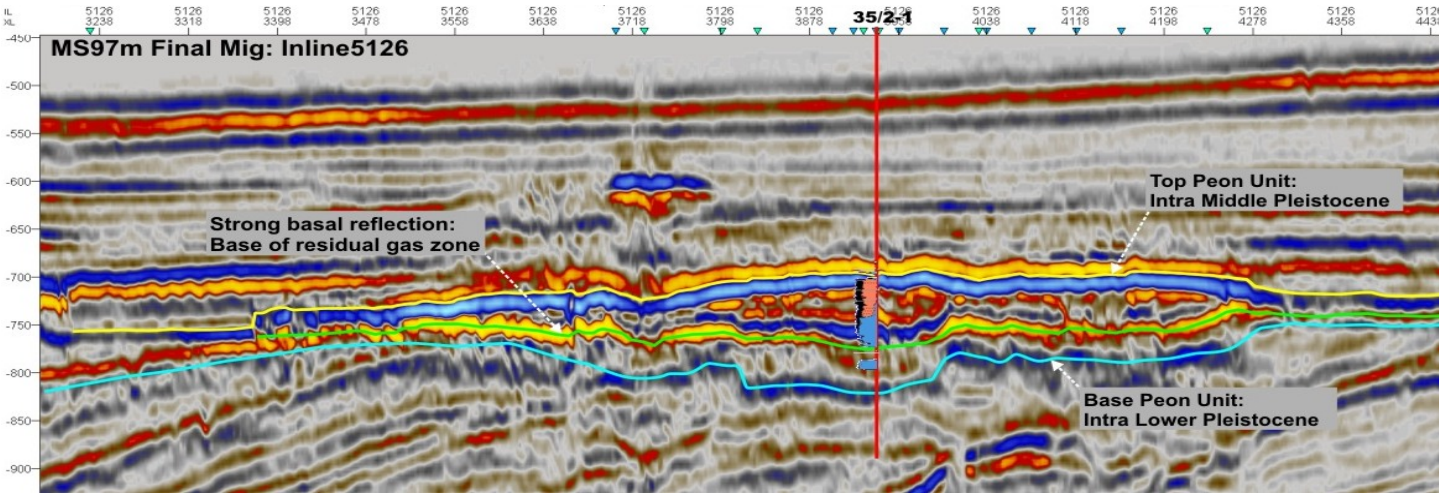

Figure 3-11 Reinterpretation of Top Peon Full Fold 3D

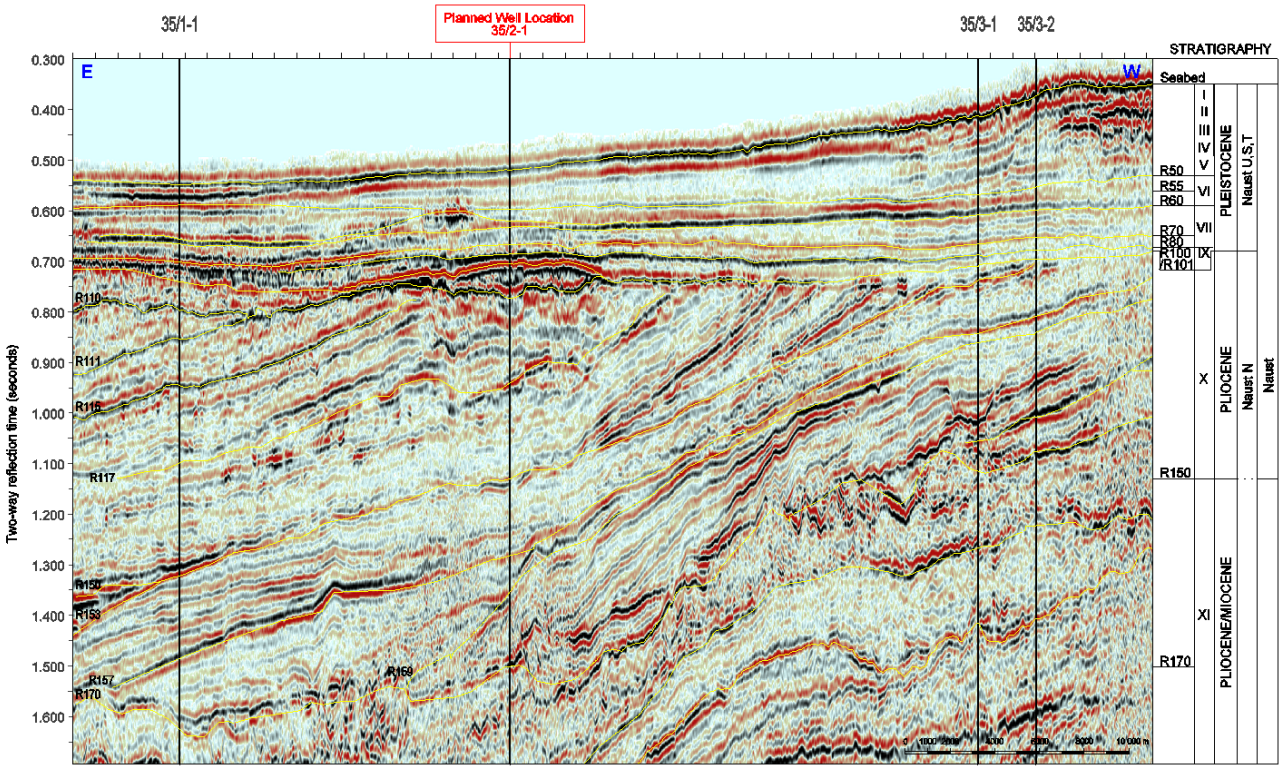

Figure 3-12 High-resolution seismic line NH0473-303 through Well 35/2-1, showing interpreted horizons and stratigraphy.

3.4 Depth Conversion

Post-drill depth conversion was performed for top and base reservoir. Peon was depth converted by the layer cake method using constant velocities. The Interval velocities were calculated from check-shot calibration:

	Interval velocities (m/s)
MSL-Seabed	1491
Seabed – Top Peon	1748
Top Peon – Base Peon	961

The top reservoir horizon was interpreted as the last continuous high amplitude event above the top reservoir. The base reservoir horizon was interpreted as the base of the low saturated gas zone. The maps were all depth shifted vertically with constant values to fit well values. The mis-ties in the maps before adjustment to the well were:

	TWT (ms)	**Depth (m)**
Seabed	-4.6	-3.4
Top Peon	5.8	9.0
Base Peon	-12.3	-8.7

4 GEOLOGICAL EVALUATION

4.1 Structural setting

Block 35/2 is located in the Sogn Graben, which is bounded by the Måløy Slope in the east, the Marflo Spur in the south and the northern tip of the Tampen Spur in the west (Figure 4-1). The Sogn Graben itself opens up towards the north from its narrow constricted geometry in block 35/2 and is in this direction bounded by the Slørebotn Subbasin, the Møre-Trøndelag Fault Complex and the Møre Basin.

The Sogn Graben is a north-south elongated basin approximately 60 km long and 20 km wide. The depth to the mapped Base Cretaceous Unconformity (BCU) varies from 4500 m in the southern part of block 35/5 to more than 8000 m in the northern part of block 35/2. The very thick Cretaceous succession within the graben constitute post-rift and thermal subsidence fill related to the Late Jurassic rifting episode.

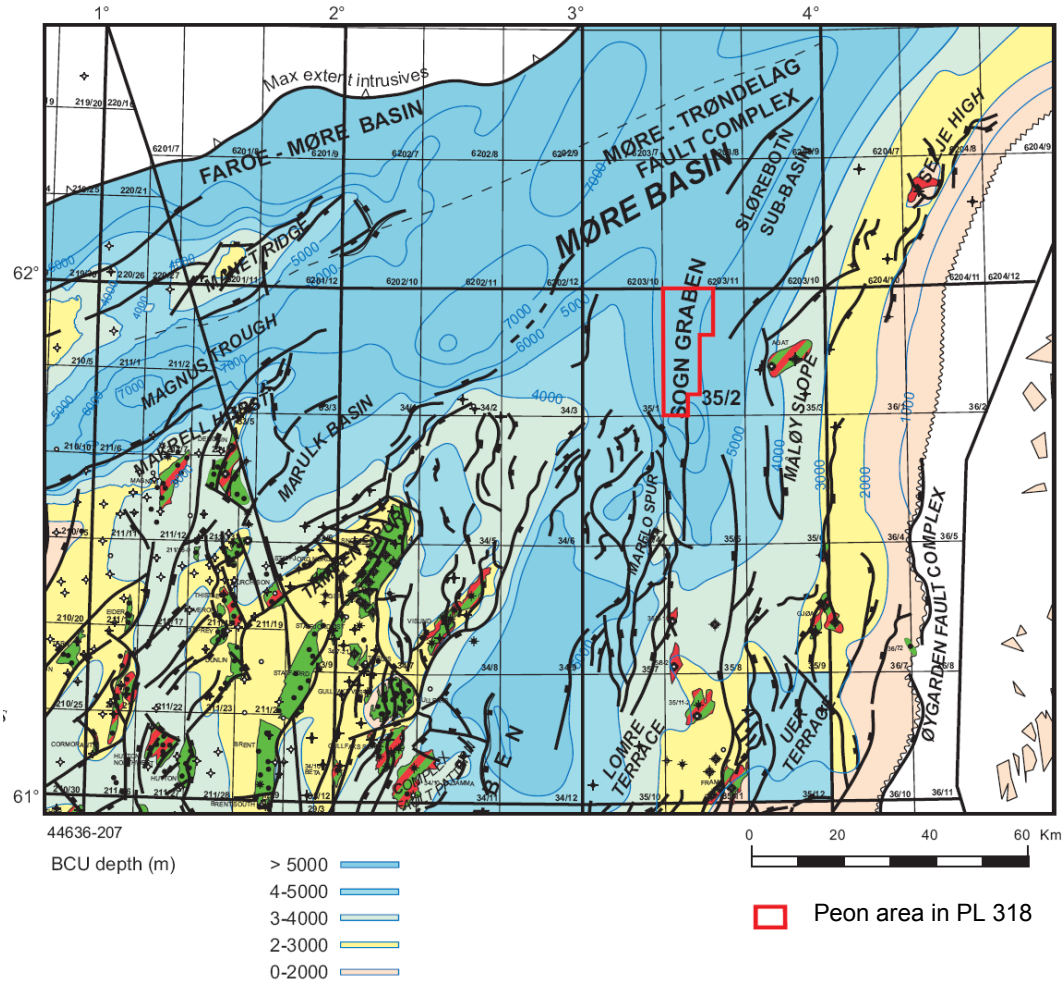

Figure 4-1. Main structural Elements northern North Sea and southern Norwegian Sea with depths to Base Cretaceous Unconformity and Hydrocarbon Fields.

4.2 Submarine Geomorphologial Features

4.2.1 Norwegian Channel

The Norwegian Channel is the most prominent seabed feature in the North Sea (**Figure 4-2**), forming a deep trough between Skagerrak continuing along the Norwegian coast for about 800 kilometres, terminating at the shelf edge north of 62°N.

The trough is deepest in Skagerrak (c. 700 m) with a shallower threshold west of Jæren (c. 270 m) from where it slopes gradually northward to the mouth at the shelf edge in about 400 m water depths. It is approximately 100 kilometres across outside Bergen, and widens towards the north reaching c. 160 kilometres at the shelf edge.

The age and origin of this trough-feature has been discussed for several decades, but there is general agreement that it bears a strong imprint of glacial erosion and deposition. The entire trough area is dominated by numerous extensive till units lying above a glacial angular unconformity found at between 100 and 200 m below seabed. The presence of large-scale glacial striations (mega flûtes oriented parallel to the trough's long axis) observed throughout this package, and a large submarine fans at the mouth of the Norwegian Channel strongly suggests that the Norwegian Channel acted as a pathway for former fast-flowing ice streams.

The ice steams drained most of the southwestern part of the Fennoscandian Ice Sheet transporting large quantities of sediments that were deposited in the Norwegian Channel, on its sides (North Sea Plateau and Måløy Plateau), and on the continental slope generating the North Sea Fan. The presence of curved seabed ridges (lateral moraines) close to the Norwegian coast (**Figure 4-2**) suggests that glaciers entering the Norwegian Channel from the western Norwegian fjords fed the ice streams.

Close to the shelf edge, a series of prominent transverse ridges, developed in till material, are found. These ridges have been interpreted as terminal moraines formed during shelf edge glaciation (King et al., 1998).

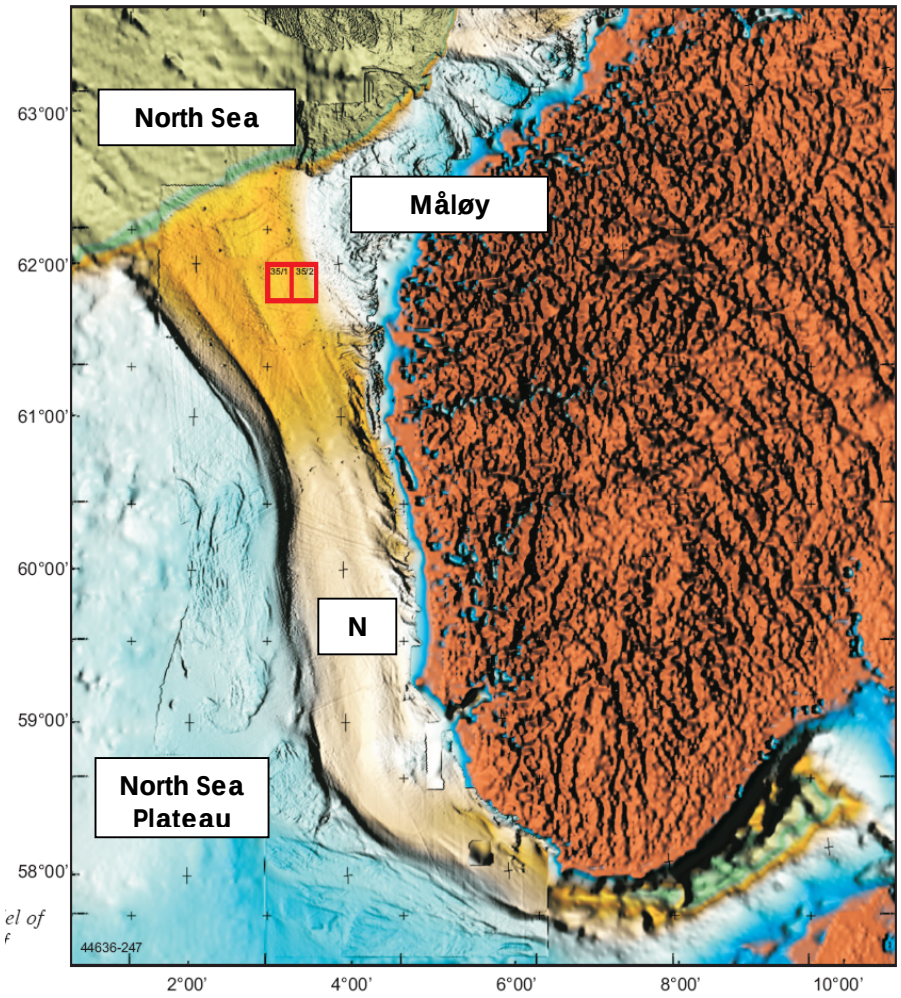

Figure 4-2. Regional shaded relief map of the seabed n the northeastern part of the North Sea. Blocks 35/1 and 35/2 are shown as red rectangles.

4.2.2 Måløy Plateau

The Måløy Plateau forms a large bank area on the eastern flank of the outer Norwegian Channel at the southwestern extension of the Møre Shelf (Figure 4-2). The water depth is c. 160 – 250 metres. The shelf is less than 60 kilometres wide offshore central Møre, but widens to 80-90 kilometres across the Måløy Plateau. The shelf edge to the north is sharply defined by the headwall of the Storegga Land-slide, a Holocene slide on the continental slope that removed parts of the outer shelf tills (Bugge, 1983; Haflidason et al., 2001). The southwestern flank of the plateau slopes less than 1° towards the Norwegian Channel. The southwestern side of the ridge is intensely iceberg scoured, while only a few scours are observed on the northeastern side.

The Måløy Plateau consists of a sequence of glacial, interglacial and deltaic sediments up to 500 m thick above the regional glacial unconformity (Nygård et al. 2002). The Norwegian Channel tills can be followed onto the Måløy Plateau. However, the Måløy Plateau has an additional, overlying 100-200 metres thick package of till and glaciomarine/deltaic sediments not present in the Norwegian Channel. The lateral

difference is most likely due to less deposition/more erosion in the channel and increased deposition in the Måløy Plateau area as a response to less dynamic ice on the bank area.

The uppermost sheet-like unit forms the base of an up to 50 metres thick composite sequence of ridges deposited towards southwest, indicated by a strong directional imprint on the seabed. The thick sequence is deposited after the collapse of the ice in the Norwegian Channel (15 ka), when the Måløy Plateau was partly deglaciated. The lack of supporting ice in the Norwegian Channel probably created a significant imbalance in the surface profile of the ice on the Møre shelf, creating a SW directed advance before the final de-glaciation of the Plateau at 12.7 ka.

4.2.3 North Sea Plateau (Tampen Area)

The northeastern part of The North Sea Plateau, the Tampen area, forms a shallow shelf area on the western side of the outer part of the Norwegian Trench (**Figure 4-2**). The area is relatively flat, dipping gently towards the north from c. 150 metres at 61°N to c. 300 metres at the shelf break. The area comprises a complex stratigraphy with flat-lying units dominated by tills that have been eroded by glaciers (ice streams) leaving several eastward sloping surfaces (former Channel flanks?).

A prominent ridge is located along the plateau edge. It is c. 100 kilometres long and 15-20 kilometres wide, comprising stiff, pebbly, sandy, silty clay (Rise et al., 1984), and was most likely deposited as a lateral moraine deposited by the Norwegian Channel Ice-stream during the last glacial maximum. It is likely that it was deposited between the fast-flowing ice and a more stagnant ice on the North Sea Plateau.

4.3 Stratigraphy

Hydrocarbons were discovered in glacial outwash sands of Pleistocene age. Details and bio-, chrono- and lithostratigraphy are provided in the sections below.

4.3.1 Biostratigraphy

Two parallel studies have been undertaken, one by the Geological Survey of Denmark and Greenland, GEUS, (dinoflagellate cyst and foraminiferal assemblages) and the other by Dr. Tor Eidvin at the Norwegian Petroleum Directorate (foraminiferal assemblages only).

Objectives

The aim of this study is to quantify the distribution of foraminifera tests and dinoflagellate cysts in order to better understand the climatic and environmental conditions during deposition of the Peon sand member.

The paleo-climate and paleo-environments are reflected by the distribution pattern and correlation with known paleontological zonations for the North Sea and Norwegian Sea.

Database

Well 35/2-1 was sampled from 546 m to 713 m (TVD RKB) with ditch cutting samples with approximately three metre intervals. In addition, four sidewall cores were obtained at 607.5 m, 613 m, 683 m and 688 m (**Table 5-1**).

GEUS have studied 57 ditch cutting samples and four sidewall cores. NPD have analysed 22 ditch cutting samples approximately 10 m apart, except just above and below the assumed Plio-/Pleistocene boundary where three metres intervals were used.

Correlation and limitations

GEUS and NPD have based their correlations on different sources:

- GEUS have based their correlation on results from ODP Hole 644B (Leg 104) located on the Vøring Plateau and Well 6404/11-1 (Riis et al. 2005) located inside the Storegga Slide Scar.
- NPD's correlation is based on foraminifera zonation in the North Sea (King 1989), North Sea and Haltenbanken (Gradstein & Bäckström 1996), Netherlands (Doppert 1980), North Atlantic (Weaver & Clement 1986) and on the Vøring Plateau (Spiegler & Jansen 1989)

Dating and correlation of sediments from well 35/2-1 was difficult as analyses mainly were based on ditch cutting samples. Caving is therefore a prominent problem masking the *in situ* flora and fauna. Further, a large proportion of particles of light material were mixed in the drilling mud (particles having the same buoyancy as foraminifera), thus diluting the fossil assemblages to the extent that the foraminifera were difficult to retrieve.

Although reworking of older taxa, caving, poor abundance and species diversity at some levels, both GEUS and NPD believe it is possible to correlate the flora/fauna in the studied section.

GEUS Results

Extensive reworking was registered throughout the analysed interval. This is in accordance with the interpreted depositional model suggesting Peon as an ice-contact / outwash deposit located at the mouth of the Norwegian Channel. An age ranging from middle Early Pleistocene to Middle Pleistocene is suggested.

The analysed section is considered to cover two interglacial periods (oceanic influence and relatively warm climate) separated by a glaciation (extreme climate and reduced oceanic impact; **Figure 4-3**). The glacial period seems to have been interrupted by a short-lived (?) interstadial/interglacial.

GEUS report a prominent unconformity at 607 m (RKB) corresponding to the base of the main sand body. This boundary seems to separate middle Early Pleistocene below and Middle Pleistocene deposits below.

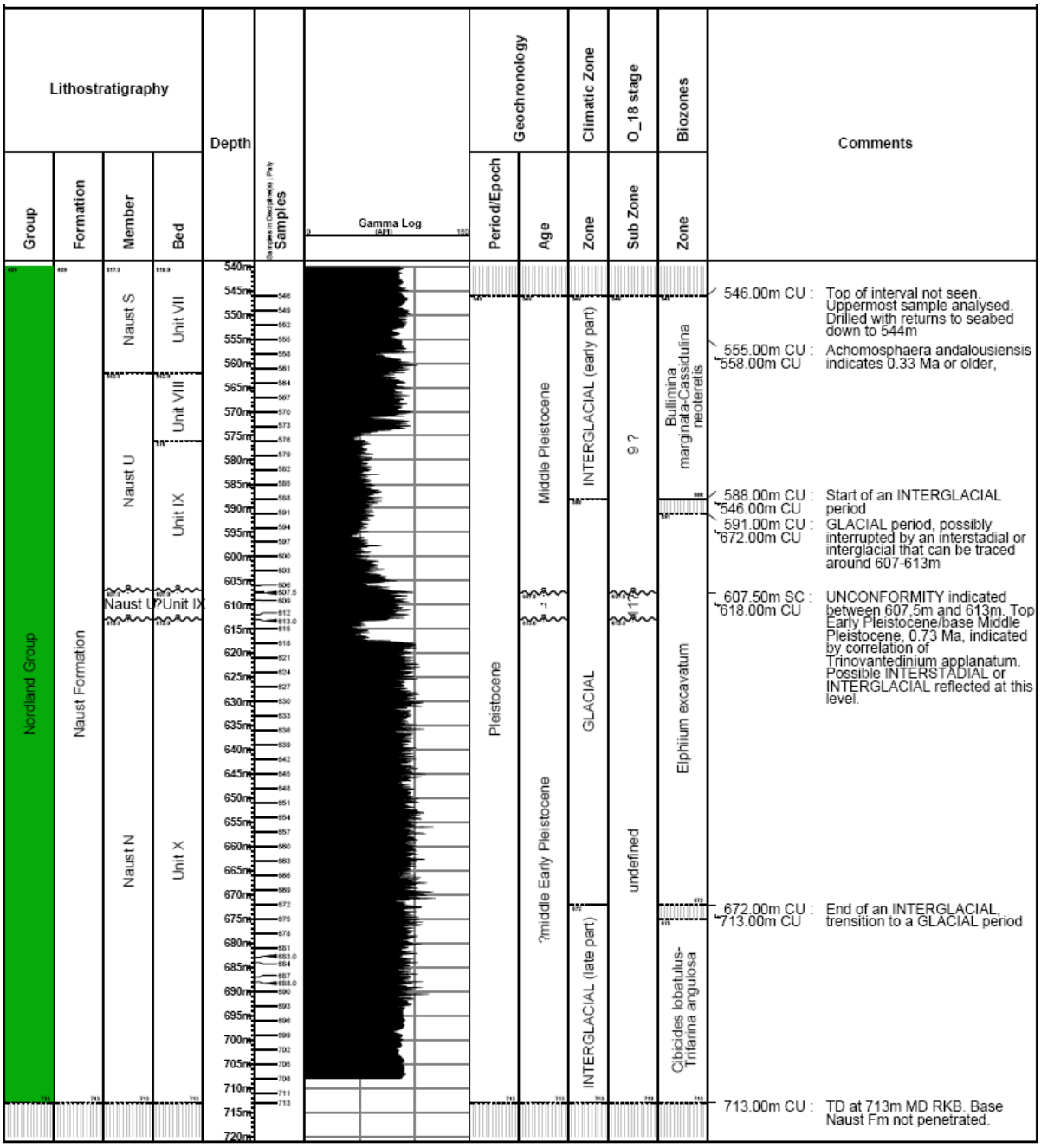

Figure 4-3. GEUS study - Biostratigraphic Summary Chart from the analysed interval, Well 35/2-1.

NPD Results

The NPD results differ from the GEUS study in that they separate the section in two and believe the deposits below Peon are older (see **Figure 4-4**):

1. Pleistocene (Nordland Group and Peon sandstone member) – 546-621m (RKB): - The age is based on benthic foraminifer *N. labradoricum* and in addition the occurrence of the planktonic foraminifer encrusted form of *N. pachyderma* (sinistral).
2. Upper Pliocene (Nordland Group) – 621-711m (RKB): - The age estimate is based on the consistent occurrence of the benthic foraminifer *E. hannai*, the consistent occurrence of the planktonic foraminifer *N. pachyderma* (dextral) and the occurrence of *N. atlantica* (sinistral). The occurrence of *N. pachyderma* (dextral) indicate a Late Pliocene age as young as approximately 1.8 Ma at 621 m, and the occurrence of *N. atlantica* (sinistral) indicate an age of approximately 2.4 Ma at 684 m.

A prominent unconformity is therefore placed at 621 m (below the sand members), representing the transition from Pliocene to Pleistocene deposits.

In Troll borehole ST8903 Sejrup et al. (1995) recorded a glacigenic diamicton immediately above an angular uncomformity, and the climatostratigraphic event corresponding to the glaciation during which this diamicton was deposited was denoted *Fedje Glaciation*. The Fedje Glaciation is correlated with the Menapian Glaciation in the Netherlands that represent the oldest evidence of a major expansion of the Fennoscandian ice sheet in form of rock fragments of Scandinavian origin (Sejrup et al., 1995; Zagwijn 1985, 1989. This suggests that the Fedje Glaciation was a regional event with a magnitude similar to the Weichselian maximum in this region (Sejrup et al, 1995).

Consequently, unless there is a specially large local erosion in the 35/2-1-area, it is likely that the ice stream witch deposited the Fedje diamicton on the Troll Field is the same as the one which deposited the sandy glacimarine depositional system in the 35/2-1 area. Detailed seismic correlation may verify this.

Further Investigations

Based on foraminiferal correlation we are only able to give a general Pleistocene age to the deposits above the angular unconformity in Well 35/2-1. Since no conventional cores are available, no palaeomagnetic investigations can be executed and no exact dating can be obtained.

However, Sejrup et al. (1995) have performed amino acid geochronology on the ST8903 core. Their investigation goes down to the Fedje Diamicton and includes normal-marine sediments that also may be present above the Peon sandstone member in Well 35/2-1. The same benthic foraminifera that Sejrup et al. (1995) have used on their analyses in core ST8903 are common above the Peon sandstone member in Well 35/2-1. Amino acid analyses of these foraminifera may prove to be an important tool for correlation with the Troll Field core. A problem is, however, that the ditch cutting samples in Well 35/2-1 may contain caved foraminiferal tests, which may hamper a correlation.

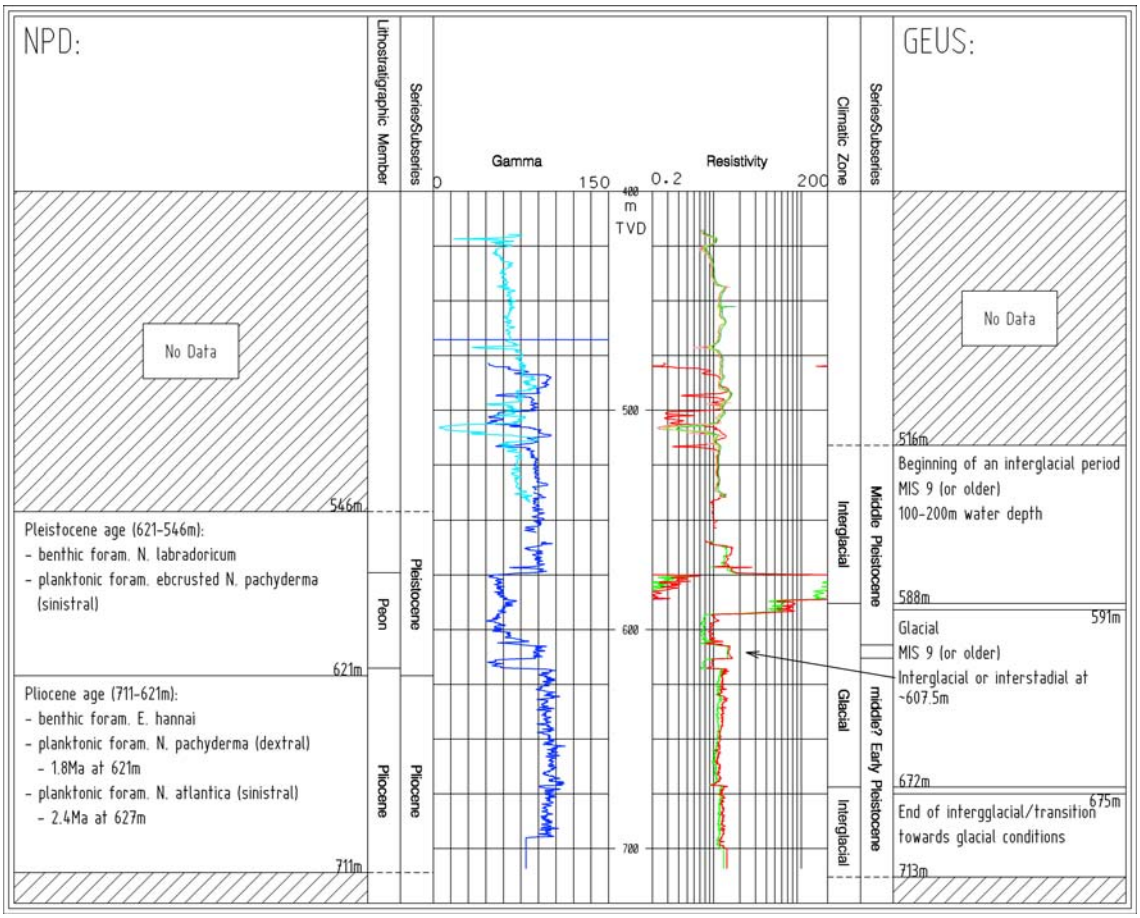

Figure 4-4. Results from the two bio-studies plotted together with LWD logs (gamma and resistivity logs).

4.3.2 Lithostratigraphy

The lithostratigraphic breakdown for well 35/2-1 is shown in **Table 4-1** and **Figure 4-5**.

Table 4-1. Lithostratigraphic breakdown of Well 35/2-1.

GROUP	FORMATION	MEMBER	SERIES/SUB-SERIES	DEPTH (m MD RKB)
Nordland	Naust T		Holocene/Pleistocene	409
		Middle to Late Pleistocene sand		493
	Naust S			484
	Naust U			562
		Peon sand		574
		Middle to Early Pleistocene sand		613
	Naust N		Pliocene	618

The Naust A Fm is missing in the well.

The reservoir section comprises Pleistocene glacial outwash sands, informally termed the Peon Sand-Member. A description of the reservoir is provided in **Section 5**. Other formations penetrated were the Naust N, U, S and T (based on stratigraphic framework suggested by the NDP Seabed Project (2004).

The **Naust N Formation** comprises CLAYS with thin sand and silt layers dipping towards the northwest. A sand layer was anticipated at approximately 782 m MSL, however this layer was not proven, as it is located below TD. The sediments above 672m RKB (unconformity) show signs of glaci-tectonics suggesting glacial conditions during or after deposition.

The **Naust U Formation** comprises the reservoir section, the thin sand member below and clay-rich till above, possibly corresponding to lithozone L6 reported by Sejrup et al. (1995).

The **Naust S Formation** comprises two units:

1. Basal unit consisting of marine clay (corresponding to lithozone L5; Sejrup et al., 1995), covered by glacial clay (corresponding to lithozone L4; Sejrup et al., 1995).
2. Upper unit dominated by sand, most likely sourced from deltas located close to the Norwegian coastline and re-deposited as NW-SE-trending sand ridges by the Norwegian Channel Ice Stream (‘mini Peon’s”).

The **Naust T Formation** comprises four well-defined clay units.

1. The basal unit represents clay-rich till, with NNW-SSE-trending flûte marks at the base and iceberg plough marks at the top. The unit correspond to lithozone L3 (Sejrup et al., 1995)
2. The till is covered by glaciomarine clay (referred to as the Eastern Trench Fm by Rise et al. 1984), not present in the Troll area.
3. The clay is covered by glacial/glaciomarine silty, sandy clay with gravel (referred to as the Norwegian Trench Fm by Rise et al. 1984), most likely deposited during the Last Glacial maximum (Late Weichselian). The unit corresponds to lithozone L2 (Sejrup et al., 1995).
4. The uppermost unit consists of very soft, to soft silty clay, deposited during the final deglaciation and post-glacial period.

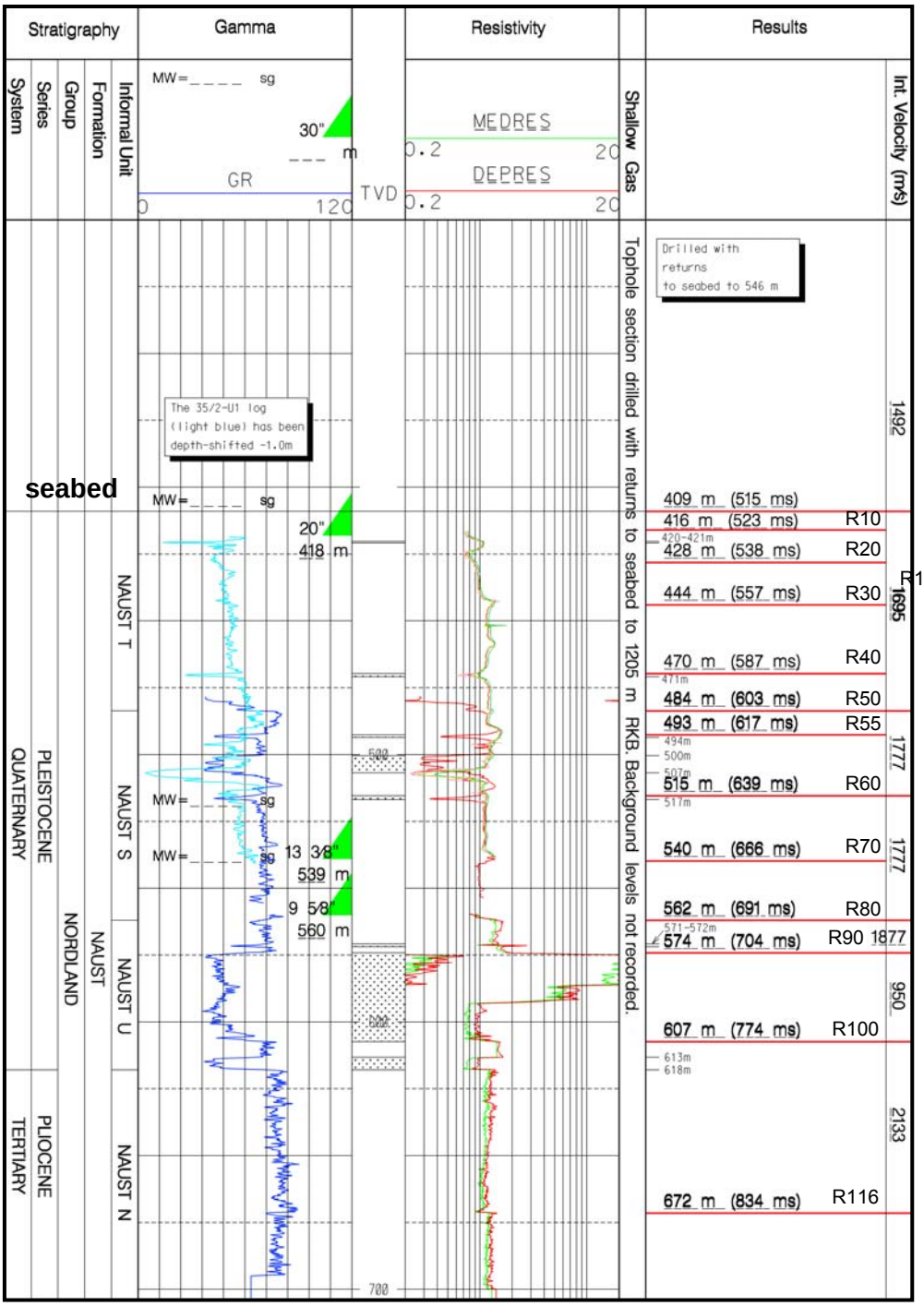

R10

Figure 4-5. Lithostratigraphic breakdown of Well 35/2-1.

4.4 Peon hydrocarbon geochemistry

Hydro's Research Centre in Bergen has performed a geochemical reservoir-study. The work is documented in **Appendix 5**. Nine Canned DC samples were sent to SINTEF for C_1-C_9 analysis. Seven gasbags samples were sent to IFE, Kjeller for isotope analysis. Cuttings samples were sent to Fluid Inclusion Technologies, Tulsa USA for fluid inclusion analysis.

Well 35/2-1 contains only dry gaseous hydrocarbons in the zone ranging from 540 to 708 m RKB MD. Gas compositions of MDT samples in the gas column, at 574-593 m RKB MD contain more than 99% methane. No liquid hydrocarbons were detected.

Table 4-2. Overview of the fluid samples and analysis.

Headspace and occluded gas in canned DC samples Analysed by SINTEF		Mud Gas from gas bags Analysed by APT as		MDT Analysed by APT as	
(m RKB MD)	Sample ID	(m RKB MD)	Sample ID	(m RKB MD)	Sample ID
543-550	1A	551	2A	587.2	3A
560-570	1B	560	2B	593	3B
570-580	1C	570	2C		
580-590	1D	582	2D		
590-600	1E	596	2E		
610-620	1G				
640-650	1H				
670-680	1I				
700-710	1J				

The presence of dry gas is confirmed by analysis of canned DC samples in the range of 550-650 m RKB MD and mud gas in the range of 551-596 RKB MD (**Figure 4-6** and **Figure 4-7**).

Carbon and deuterium isotope values of methane in MDT samples at 587 and 593 are by average –73 and –211, respectively. The carbon isotope values for methane in mud gases at 551-596 m RKB MD support the results for the MDT samples. The gaseous hydrocarbons therefore show signs of a biogenic origin. The top sealing and reservoir zones at 551-596 m RKB show a uniform gas column. **Table 4-3** shows the $\delta^{13}CH_4$ (methane) values. **Figure 4-8** shows the classification of carbon and hydrogen isotopes values.

Oil traces on MDT dump chamber and mud samples at 570, 590 and 610 m RKB MD shows traces of hydrocarbons. The well is drilled by a water-based mud system. These oils are enriched in C_{12-16} hydrocarbons, suggesting a refined product of unknown origin.

Fluid inclusion study of this shallow well shows a low number of inclusions**. Figure 4-9** Enhanced concentrations of both saturated and aromatic hydrocarbons above 630 m indicate a seal at this depth. Alternatively, a dramatic shift in porosity or mineralogy may enhance the inclusion density and consequently hydrocarbon enrichment.

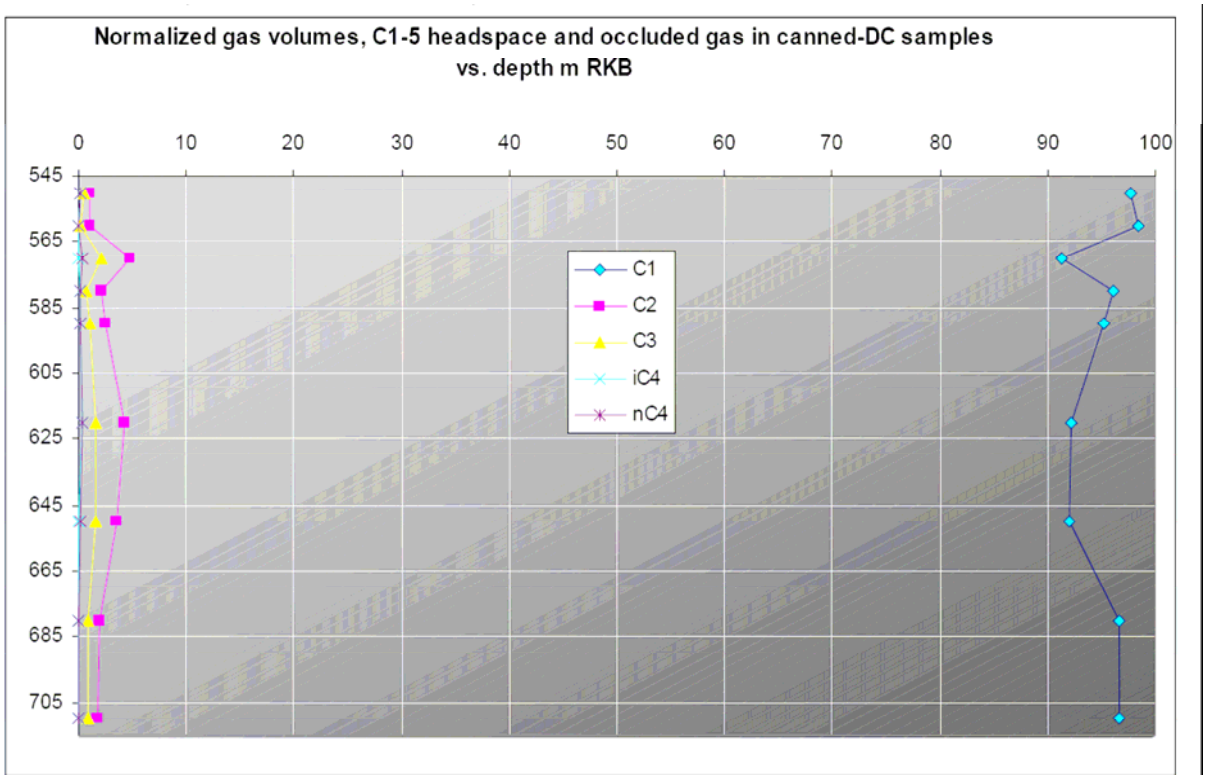

Figure 4-6. Composition, headspace and occluded gas.

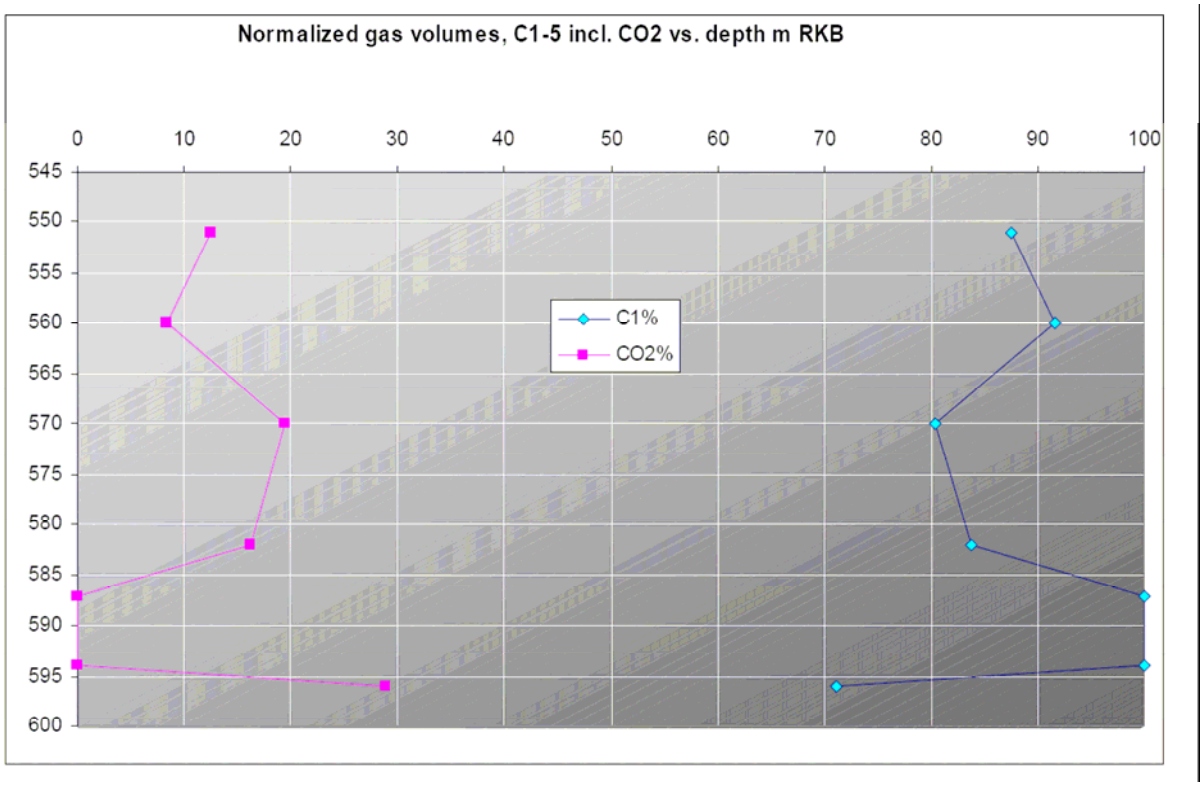

Figure 4-7. Gas composition in the mud gas shows the amount of Methane and CO2. The relative amount of C2+ hydrocarbons is less then 0.05 vol%.

Table 4-3. Results from the Isotope analysis.

Sample depth	Sample ID	Sample Type	C1d13C	Deuterium
551	2A	Gas bag	-74.8	
560	2B	Gas bag	-74.7	
570	2C	Gas Bag	-73.8	
582	2D	Gas Bag	-73.6	
596	2E	Gas Bag	not enough	
587.2	3A	MDT	-72.7	-211
593	3B	MDT	-72.6	-210

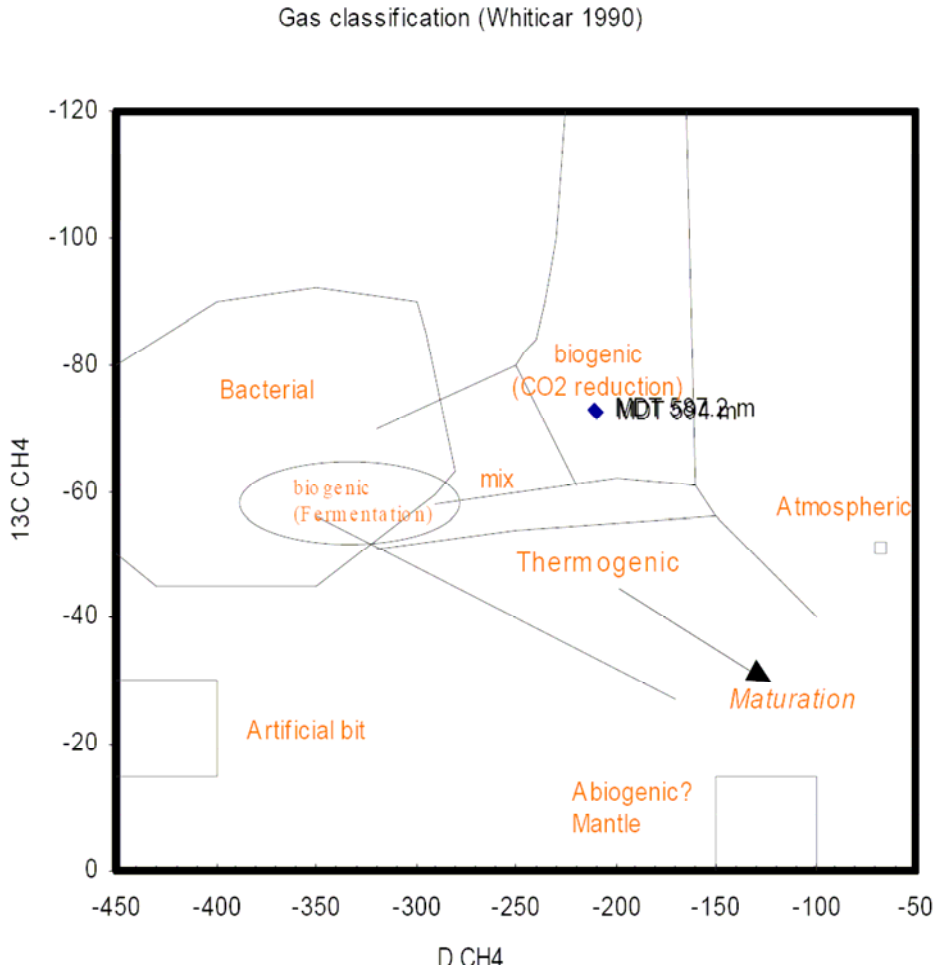

Figure 4-8. Classification using carbon and hydrogen isotope values.

The Fluid inclusion study indicates that the well section above 570 m is generally low in hydrocarbons. The section 585 - 630 m is enhanced in saturated and aromatic hydrocarbons. The entire analysed section of 550 - 712 m constrains traces of sulphur compounds. Access to sulphur compounds indicates biogenic activity by sulphate reduction. Gaseous hydrocarbons probably originated from biogenic processes.

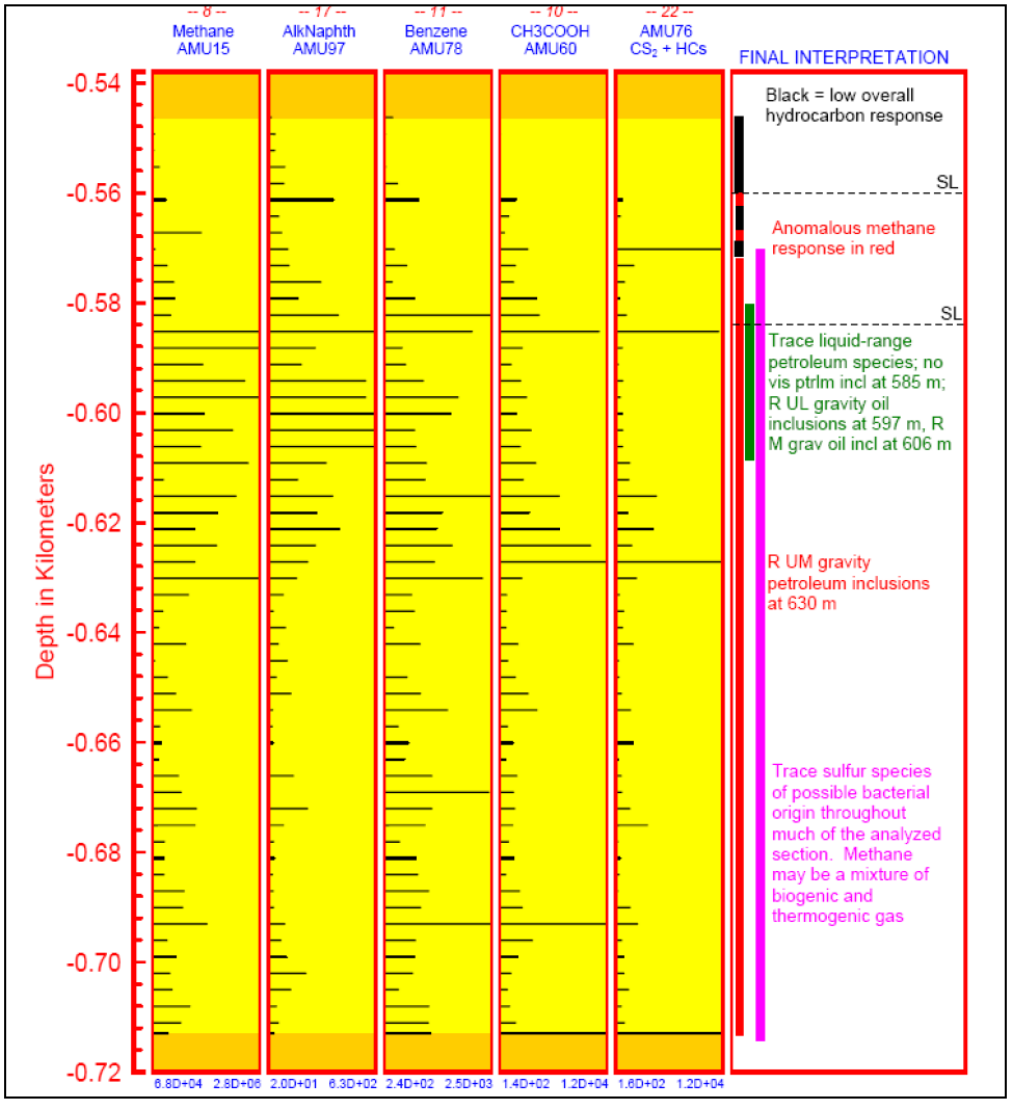

Figure 4-9. FIS summary.

4.5 Hydrocarbon migration/diffusion

The dry gas accumulation in Peon is mainly of biogenic origin. This is a result of bacterial gas that occurs in a depositional setting with high sedimentation rate and low geothermal gradient. The high sedimentation rate has in this region a twofold effect namely the preservation of organic matter throughout the sedimentary section and prevention of escape of shallow gas.

The possible traces of the thermogenic input are likely to be a result of re-migrated trapped gas within Jurassic structures. The hydrocarbons are generated by the deeply buried kitchen e.g. Draupne Fm. located west of the structure

5 RESERVOIR DESCRIPTION

5.1 Introduction

The Peon Reservoir comprises a massive sand body of middle Pleistocene age. The sand interval consists of two coarsening-up units, as indicated by the gamma log and high-resolution seismic. A second sand layer, approximately 8 metres below the reservoir is not regarded as part of the reservoir. However, it represents an important boundary, separating dipping Pliocene and sub-horizontal Pleistocene-to-Holocene units.

The reservoir quality of the sands is confirmed to be good (at least in the central part of the sand body). The well logs indicate an average porosity of 33.2%, however no direct permeability-measurements were possible as no cores were obtained.

The following studies show that glacial processes have dominated the whole well section with no indications for a true ice-distal, marine dominated environment. Still the age control is poor and two independent studies show quite different results.

5.2 Samples from well

Table 5-1 shows the various samples obtained from Well 35/2-1.

Table 5-1. Samples from well

Type	Depth (m RKB)	Type	Depth (m RKB)	Type	Depth (m RKB)	Type	Depth (m RKB)
DC	576	DCG	630	DCPA	618	FLUI	587.2
DC	579	DCG	640	DCPA	624	FLUI	594
DC	582	DCG	650	DCPA	627	GASB	551
DC	585	DCG	660	DCPA	630	GASB	560
DC	588	DCG	670	DCPA	633	GASB	570
DC	588	DCG	680	DCPA	636	GASB	582
DC	591	DCG	690	DCPA	639	GASB	596
DC	594	DCG	700	DCPA	642	GASB	603
DC	597	DCG	710	DCPA	645	GASB	615
DC	600	DCG	713	DCPA	648	GASB	625
DC	603	DCPA	546	DCPA	651	GASB	630
DC	603	DCPA	549	DCPA	654	GASB	641
DC	606	DCPA	552	DCPA	657	GASB	650
DC	615	DCPA	555	DCPA	660	GASB	665.5
DC	618	DCPA	558	DCPA	663	GASB	679
DC	621	DCPA	561	DCPA	666	GASB	688.5
DC	624	DCPA	564	DCPA	669	GASB	700
DC	627	DCPA	567	DCPA	672	GASB	710
DC	630	DCPA	570	DCPA	675	GASB	713
DC	633	DCPA	573	DCPA	678	GASB	713
DC	636	DCPA	576	DCPA	681	MUD	550
DC	639	DCPA	579	DCPA	684	MUD	570
DC	642	DCPA	582	DCPA	687	MUD	590
DC	681	DCPA	585	DCPA	688	MUD	610

Type	Depth (m RKB)	Type	Depth (m RKB)	Type	Depth (m RKB)	Type	Depth (m RKB)
DC	684	DCPA	588	DCPA	690	MUD	630
DC	687	DCPA	591	DCPA	693	MUD	650
DC	690	DCPA	594	DCPA	696	MUD	650
DC	693	DCPA	597	DCPA	699	MUD	670
DCG	550	DCPA	600	DCPA	702	MUD	690
DCG	560	DCPA	603	DCPA	703	MUD	710
DCG	570	DCPA	606	DCPA	705	MUD	713
DCG	580	DCPA	607.5	DCPA	708	MUD	713
DCG	590	DCPA	609	DCPA	711	SWC	607.5
DCG	600	DCPA	612	DCPA	713	SWC	613
DCG	610	DCPA	615	DCW	660	SWC	683
DCG	620	DCPA	617	DCW	713	SWC	688

DC: Drill cuttings; DCG: Drill cuttings, canned geochemical sample; DCPA: Drill Cuttings, Palyno-slide; DCW: Drill cuttings unwashed; FLUI: Fluid sample, unspecified; GASB: Gas from mud flow “sniffer”, bag; MUD: Mud sample; SWC: Sidewall core

5.3 Petrography, mineralogy and grain size

Hydro’s Research Centre performed a petrographical analysis of drill cuttings and sidewall cores from Well 35/21. The study covers the reservoir section and the clay below and comprises thin section- and X-ray analyses. The database is listed in Table 5-2. Sample depths given are driller's depths (m RKB).

The mineralogical composition, based on quartz, feldspar and lithics, and the clay composition is very uniform for the analysed samples from the reservoir. The signature of the clay mineral assemblage below the reservoir is similar to that in the reservoir section, but what looks like mica in the reservoir seems to be more illitic in the silt/shale section. There is no significant smectitic component in the reservoir or below, thus the illitic component might well be altered mica.

Table 5-2. Petrographical database for Well 35/2-1. No porosity and permeability measurements have been performed due to the nature of the samples.

Depth m (RKB)	Sample Type	Thin Section	X-Ray Bulk
576.00	DC	X	X
579.00	DC	X	X
582.00	DC	X	X
585.00	DC	X	X
588.00	DC	X	X
591.00	DC		X
594.00	DC	X	X
597.00	DC	X	X
600.00	DC	X	X
603.00	DC		X
606.00	DC	X	X
607.50	SWC	X	X

613.00	DC		X
615.00	DC	X	X
618.00	DC	X	X
621.00	DC	X	X
624.00	DC		X
627.00	DC		X
630.00	DC		X
633.00	DC		X
636.00	DC		X
639.00	DC		X
642.00	DC		X
681.00	DC		X
683.00	SWC	X	X
684.00	DC		X
687.00	DC		X
688.00	SWC	X	X
690.00	DC		X
693.00	DC		X

5.3.1 Preparation and Limitations

Thin section analysis: - Thin sections were prepared from 14 samples (11 drill cuttings samples [DC] and 3 sidewall cores [SWC]). Various colour-staining techniques were performed in order to detect important minerals. **Figure 3-1** and **Figure 5-2** show the composition of the near top and near base reservoir, respectively.

The dominant grain size is expressed as the average diameter in millimetres of 10 representative grains. Sorting has been estimated by visual comparison of the microscope image with four standard sorting patterns.

As the reservoir sand is un-lithified, some of the matrix may have been washed out during the washing-and-drying process, not allowing porosity-determination. Furthermore, the grains may have been crushed during the drilling process.
The porosity or permeability measurements are therefore not reliable as no in situ samples were obtained (i.e. the reservoir consists of loose sand).

XRD analysis: - The bulk mineralogy of 22 DC- and four SWC samples was analysed using X-ray diffraction (XRD). The results were compared with 135 sample-mixtures from 14 mineral standards in order to identify and quantify the mineral composition. The standards are believed to represent relevant sandstone reservoir samples.

It is believed that most of the clays in the DC samples may have been washed out, and the SWC samples are contaminated by drilling-mud. For these reasons, and because of very low clay content, no clay fraction analyses were performed.

Due to the poor quality of the samples it is difficult to compare the thin section- and XRD analyses. Contaminating minerals, such as sylvite (KCl), halite (NaCl) and barite were not counted, only analysed using XRD. Further, these minerals were not calibrated producing outliers in the calibration model for the most severely contaminated samples.

In spite of the poor sample quality, Hydro's Research Centre has chosen to present the XRD data, as they seem reasonable. Still, the results should be regarded as estimated values.

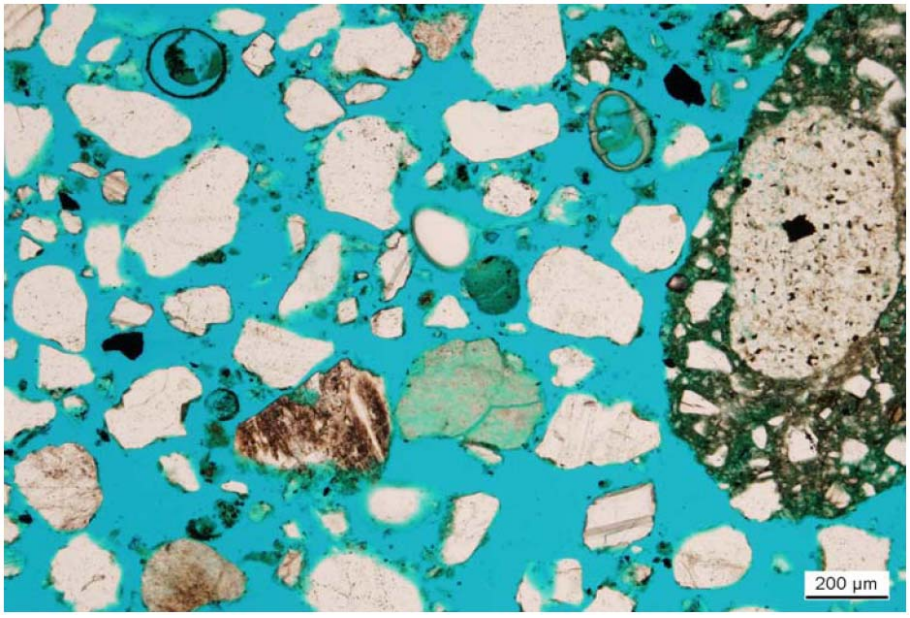

Figure 5-1. Thin section from near top reservoir (576m RKB) showing quartz (44%), feldspar (15%), rock fragments (9%), carbonate (21%) and other minerals (11%). Blue colour: pore volume.

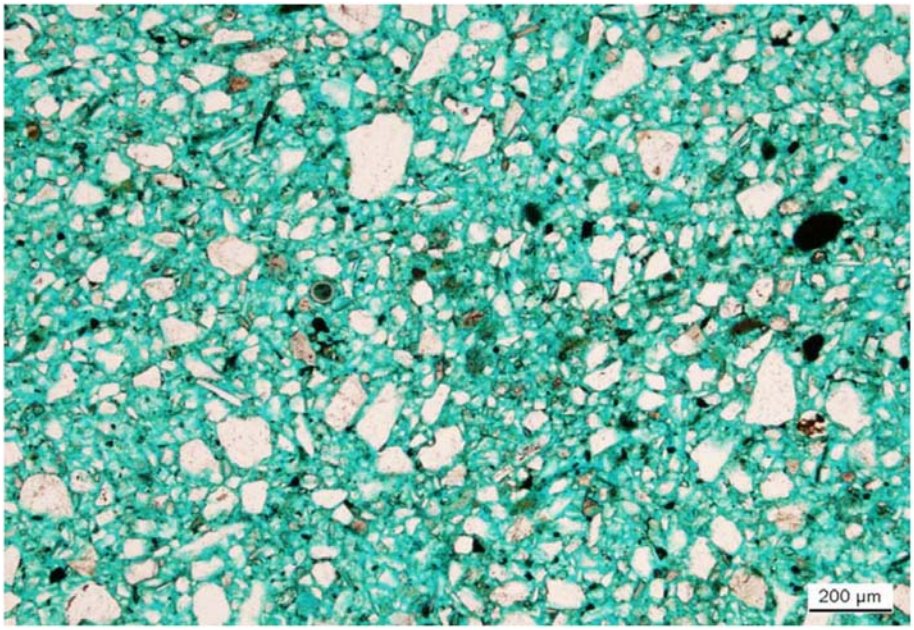

Figure 5-2. Thin section from near base reservoir (607.5m RKB) showing quartz (36%), feldspar (10%), mica (4%), rock fragments (1%), carbonate (1%) and other minerals (6.5%).

5.3.2 Observations

The reservoir samples (i.e. above 621m RKB) are dominated by quartz (~35-65%). The quartz totally dominates feldspar and lithic fragments (Figure 5-3), and the composition is

rather uniform throughout. The grain size is medium in most samples and the sorting ranges from moderate to good.

The cement content ranges quite a lot (~2.5% - ~25%), clearly reflecting the quality of the samples and harsh depositional environment. Thin sections suggest calcite cement, however the XRD analysis show small amounts dolomite or ankerite.

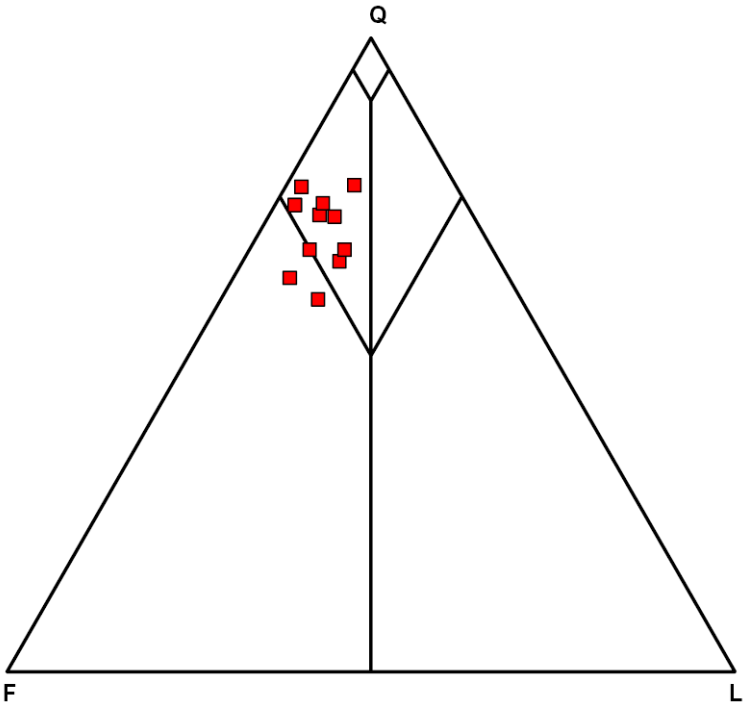

Figure 5-3. Composition of Quartz feldspar and lithic fragments (point counted samples).

The section below the reservoir is dominated by clay. The clay mineral composition is similar to the reservoir section, but what seems to be mica in the reservoir seems to be more illithic in the section below.

The share of clay minerals seems to increase with depth (relative to the quartz content), probably caused by increased illite, chlorite (mixed layer clays) and kaolinite. Smectite is not present, thus the illite is most likely altered mica (glacial erosion rather than weathering).

Conclusions:

- The distribution of quartz, feldspar and lithic minerals, as well as the clay composition is uniform throughout the reservoir section. This indicates:
  1. One dominant transport/depositional mechanism
  2. Single source; either long-transported well-sorted sand or re-deposited older sands (Eocene-Miocene)
- The clay mineral composition below the reservoir sand suggest glacial conditions throughout (i.e. glacial erosion rather than weathering)

5.4 FMI Analysis

Since the pre-drill conceptual, geological model of Peon suggested that it is a glaciogenic feature, possibly deposited close to the ice front, it was believed that the FMI log should reveal typical ice-contact depositional features in addition to sediment deformation due to subsequent ice movement.

Eriksfiord AS performed the FMI analysis, covering a 150 metres long interval, between 556 metres and 706 metres (below RKB; Figure 5-4).

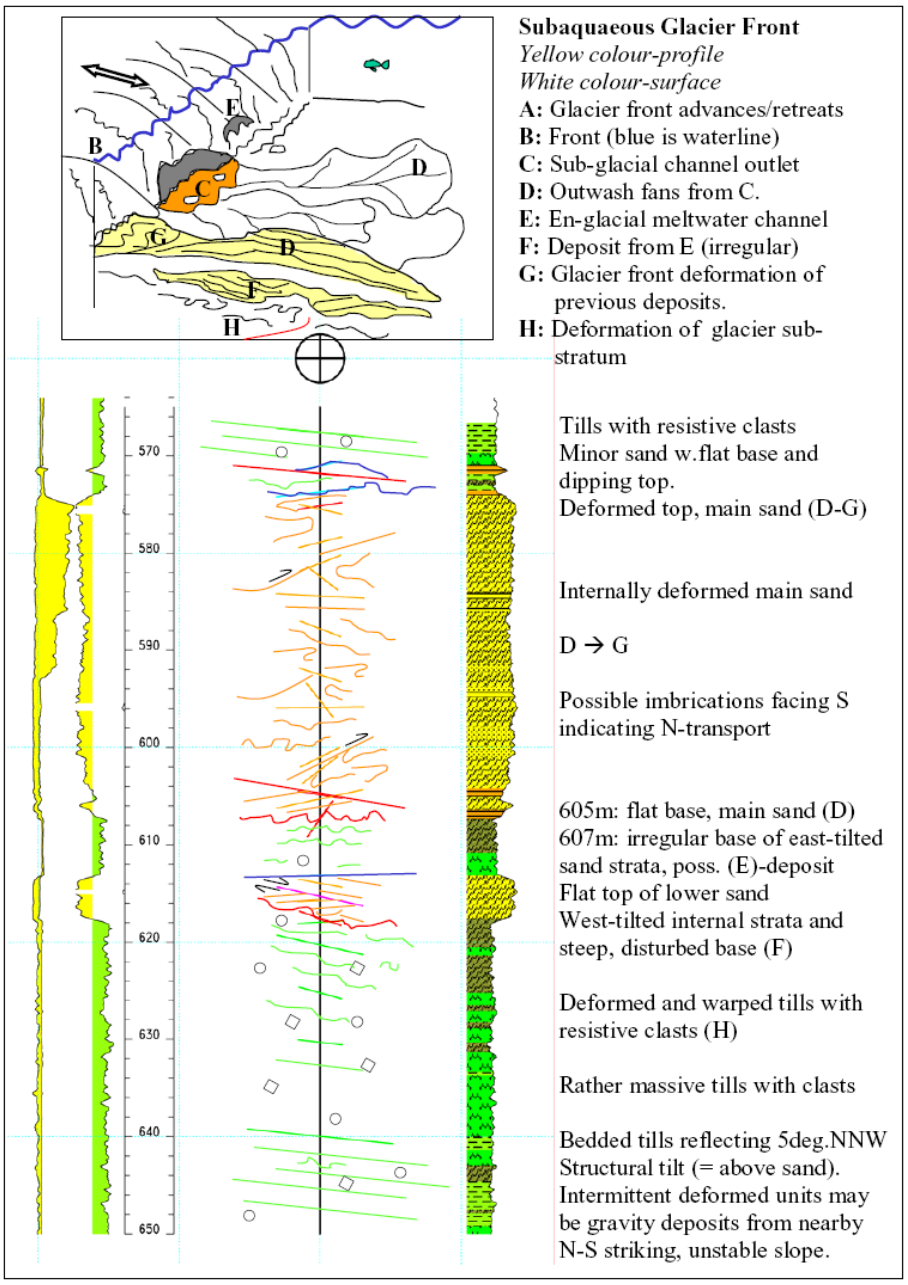

Figure 5-4. Conceptual sketch of sub-aqueous ice-stream front with various deposits and structures and suggested corrections to Peon features interpreted from FMI image logs (simplified).

Structural tilt estimations subdivided the well in four zones with a mean bedding tilt of 5°, ranging between 4.4° and 14°. The main trend is a shallow NW-NNW structural tilt with one or two possible minor unconformities at 653 and 605m.

The succession begins with the lower muds showing a resistive spotted texture. The resistive bodies can be explained in different ways such as carbonate fossils or nodules or siliciclastic clasts. The latter seems most likely, as glaciers were present at or near the site, providing coarse fragments to the continental slope. The sediments most likely originated from gravity flows triggered by over-steepened slope or formed *in-situ* due to heavy "rain-out" of clasts from melting icebergs close to the ice front. Increased deformation above 631m may reflect disturbance and warping beneath an advancing ice front.

The transition from the mud-dominated lower part to the sand-dominated upper part (i.e. above 621 metres) is probably caused by a shift from ice-distal to ice-proximal conditions (e.g. onset of ice streams). The interval including the lower sand to the lowermost upper sand may represent englacial / supraglacial crevasses and/or ice-pocket fills with a steeply dipping base and unimodal, semi-horizontal stratification. After the ice melted, they were deposited at variable tilting angles on the deformed substratum.

The upper sand (between 605 and 574m) is characterized by E-W striking axial trends and is interpreted as a sub-aqueous outwash fan. The sedimentation took place at a slight distance from the grounding line by traction or by settling from sediment-loaded melt water underflows. The subsequent soft-sediment deformation can be attributed to ice push with a suggested transport direction to the N or NW. Ice stream advances resulted in internal folding, thrusting and imbrications, governed by transversal deformation axes.

In conclusion, glacial processes appear to dominate the whole well section with no indications for a true ice-distal, marine-dominated environment. Fluvial sands were never deposited or they have not been preserved in Well 35/2-1.

5.5 Depositional model

5.5.1 Pre-drilling Assumptions

Prior to drilling, Peon was regarded as an ice-contact / outwash deposit located at the mouth of the Norwegian Channel (**Figure 5-5**).

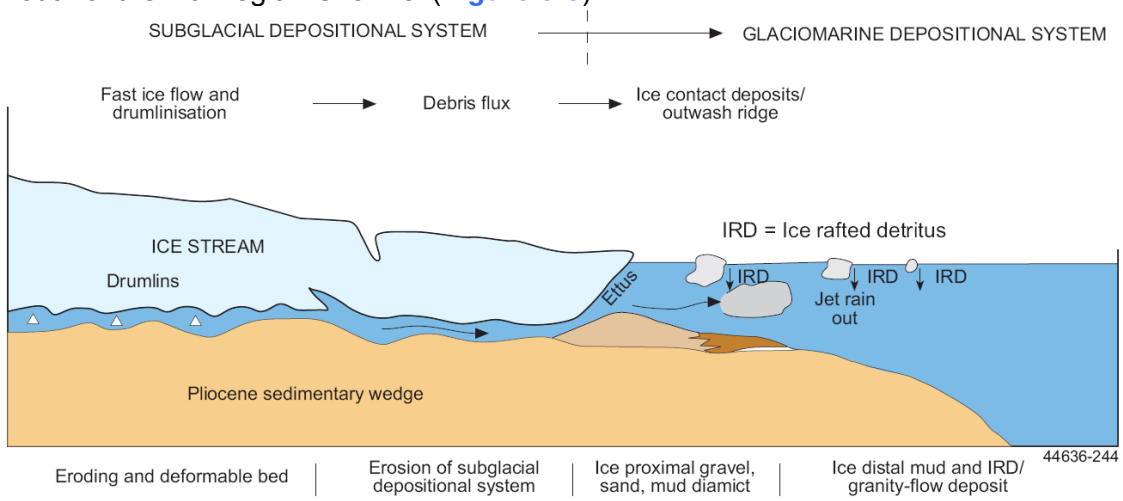

Figure 5-5. The sketch shows the Peon Depositional Model: Relationship between fast ice flow and feeding sub-glacial sediment (i.e. sand) to the ice margin (modified after McCabe et al., 2005).

It is known that the Norwegian Channel acted as a pathway for fast moving ice streams during glaciations since 1-0.5 Ma, and we believe that ice streams generated the boundary (erosional surface) separating the Pliocene (early Pleistocene?) progradational strata from the overlying sub-horizontal units of till and glacial-marine/normal marine clays.

The Norwegian Channel has therefore acted as a major confluence area for ice and melt-water during the Late Plio-Pleistocene, and most of the ice and water generated by the Scandinavian Ice Sheet were funnelled into the low-lying area of the Norwegian Channel and discharged at the channel-mouth. The result is the large submarine fan deposited in front of the Norwegian Channel, consisting of an up to 1800 m thick Late Plio-Pleistocene sedimentary wedge (Nilson, 1996).

It is assumed that large quantities of sand was exposed in Norwegian Channel region when the first ice streams were developed, and the sand could have easily been eroded and re-deposited by glaciers, not directly by the ice but through glacial-fluvial processes (sub-glacial rivers?).

Peon displays some of the features commonly associated with fluvial ice contact and sub-aqueous outwash deposits, e.g. steep ice-contact slopes typical for fluvial ice contact deposits, and lack of topset beds typical for sub-aqueous outwash deposits. However, the poor resolution of the existing 3D seismic does not allow us to observe many of other features related to such deposits (e.g. collapse structures and foreset beds).

Peon's position (e.g. at the palaeo shelf edge) suggests that melt water generated by the Scandinavian Ice Sheet was funnelled through one or more channels either englacial or sub-glacial into the low-lying area of the Norwegian Channel and discharged at the ice front.

5.5.2 Post-well studies

The following key observations obtained during the post-well analyses support the current depositional model:

- The FMI study concludes that glacial processes appear to dominate the whole well section with no indications for true ice-distal, marine-dominated environment.
- The paleontological analyses show extensive reworking throughout the sampled interval, which is expected if glacial processes dominate.
- A prominent unconformity has been suggested at 621m (i.e. below the lowermost sand). The sediments above are most likely of Pleistocene age, while the sediments below may be of Late Pliocene to Early Pleistocene age, but no exact dating were obtained as no palaeomagnetic investigations could be executed.
- The formainiferal fauna suggests that he clays beneath the unconformity span the end of an interglacial period (below 675 m) and a glacial period (above 675m). However, the presence of illite suggests glacial conditions throughout since illite normally is a product of physical weathering and glacial scour, particularly of crystalline rocks, such as those that are widespread in Norway. The lack of depth-trend demonstrates stable erosion of these rock types, suggesting that glaciers were present onshore throughout.
- The FMI study suggests that the reservoir sands were deposited by traction or by settling from sediment-loaded melt water underflows (i.e. high-density flows). This is in agreement with the grain-size distribution, sorting and mineral assemblage. The

subsequent soft-sediment deformation can be attributed to ice-push with a suggested transport direction to the N and NW.

- The reservoir sand being dominated by quartz, is in agreement with the source being the Oligocene-to-Eocene sands to the S/SE (i.e. re-deposition of well-sorted sands)
- GEUS suggest that the clays immediately overlying the reservoir sands were deposited during Marine Isotope Stage 9 (0.3-0.4 Ma), however this does not fit with the seismic correlation, suggesting MIS 13 or older (i.e. between 0.5 and 1 Ma).

6 FORMATION EVALUATION

6.1 Log data acquisition and quality

6.1.1 LWD Logs

Baker provided the MWD/LWD services for the well 35/2-1, according to Table 6-1. The data are of good quality

Table 6-1. MWD/LWD services run in well 35/2-1.

Run	Section	Sensors	Interval logged (MD RKB)	Comments
1	9 7/8	GR-RES-ECD*DIR	409.0 - 544.0 m	Pilot
2	36	GR-RES-ECD-DIR	409.0 - 463.0 m	Hole opener – broken drill string
3	36	GR-RES-ECD-DIR	409.0 - 483.0 m	Respud
4	17½	GR-RES-ECD-DIR	483.0 - 543.0 m	Section TD
5	12¼	GR-RES-ECD-DIR	543.0 - 561.0 m	Section TD
6	8½	GR-RES-ECD-DEN-NEU-TesTrak	561.0 - 586.0 m	LWD failure
7	8½	GR-RES-ECD-DEN-NEU-TesTrak	586.0 – 713.0 m	TD

*:ECD: Circulating Density tool

6.1.2 Wire line Logs

The wire line logs are summarized in Table 6-2. Schlumberger provided the wire line services for Well 35/2-1. The data are of good quality, except from the sidewall cores, MRCT. The recoveries for the MRCT runs were poor. The few “recovered” samples were not fit for analysis.

Table 6-2. Wire line services run in well 35/2-1.

Run #	Section	Tool String	Interval logged (MD RKB)	Comments
1A	8½	FMI-MSIP**	484.0 - 707.0 m	MSIP chosen (with success!) due to very slow FM
1A	8½	MDT	576.0 - 612.0 m	Pressure points and samples. Got stuck; skipped 3 deepest pressure points
1A	8½	SP-HRLA-PEX-ECS*	550.0 - 709.0 m	HRLA failed
1A	8½	VSI	430.0 – 612.0 m	Station every 10m
1A	8½	MRCT***	613.0 – 703.0 m	Tool failure. 8 cores, 3 “recovered”
1B	8½	SP-HRLA	560.0 – 709.0 m	HRLA rerun
1B	8½	MRCT	575.0 – 607.5 m	23 cores, 1 recovered

1C	8½	MRCT	571.0 – 574.0 m	3 cores, 0 recovered
1D	8½	MRCT	578.0 – 614.0 m	5 cores, 0 recovered

*: ECS: Mineral lithology tool
**: MSIP- also called Sonic Scanner (New & promising SLB sonic tool.)
***: MRCT: Sidewall core plugs

6.2 Pressure measurements

16 MDT pressure tests were attempted during MDT run 1A, of which 13 are considered successful. 2 tests were dry and 1 was supercharged. Two of the good tests were gathered during sampling (one at 582m MD and one at 589m MD). In general, the pressure tests are of good quality.

6.2.1 Pressure Points

16 MDT pressure tests were attempted during MDT run 1A, of which 13 are considered successful. 2 tests were dry and 1 was supercharged. 2 of the good tests were gathered during sampling (one at 582 m and one at 589 m).

See **Table 6-3** for listing of results from the MDT pressure test including Formation Pressure (Quartz Guage) in bar together with initial hydrostatic pressure (HYDB) and final hydrostatic pressure (HYBA) in bar.

Table 6-3. Listing of MDT pressure tests.

DEPTH M MD RKB	DEPTH TVD MSL	FMP (QG)	HYDB	HYDA	MOBILITY [MD/CP]	COMMENT
574.9	549.9		66.031	66.031	-	Dry test
576.0	551.0	59.704	66.416	66.400	-	Supercharged
577.6	552.6		66.307	66.307	-	Dry test
580.0	555.0	59.665	66.858	66.858	487.4	O.K.
582.0	557.0	59.703	67.134	67.065	1029.0	O.K.
582.0	557.0	59.695	67.065	67.203	220.2	O.K.
583.0	558.0	59.673	67.203	67.203	960.1	O.K.
586.5	561.0	59.685	67.617	67.617	695.7	O.K.
589.0	564.0	59.738	67.892	67.892	380.0	O.K.
589.0	564.0	59.707	67.892	67.892	547.9	O.K.
591.0	566.0	59.716	68.375	68.375	1050.4	O.K.
593.0	568.0	59.746	68.099	68.099	509.2	O.K.
596.0	571.0	60.047	68.720	68.720	2700.9	O.K.
598.0	573.0	60.253	68.927	68.927	66.5	O.K.
602.0	577.0	60.646	69.409	69.409	200.5	O.K.
602.0	577.0	60.663	69.409	69.409	97.6	O.K.

6.3 Gas PVT analysis

Fluids from the gas zone were successfully samples and analysed. This includes MDT fluid samples, gasbags and canned drilled cuttings.

Table 6-4. List of sample types and depth taken for gas analysis

Gasbags	MUD	MDT
551	550	587.2
560	570	594
570	590	
582	610	
596	630	
603	650	
615	670	
625	690	
630	710	
641	713	
650		
665.5		
679		
688.5		
700		
710		
713		

Table 6-5. Normalised values from the manual injection of the gas from run 1A MDT 35/2-1 at 589 m RKB MD depth performed at the rig. The MDT material was sent to PVT analysis at Norsk Hydro Research Centre in Bergen.

	C1	C2	C3	iC4	nC4	iC5	nC5
SC#43 - 1	99.37	0.12	0.08	0.07	0.09	0.12	0.15
repeat	99.26	0.12	0.08	0.08	0.11	0.15	0.19
SC#43 - 2	99.96	0.00	0.01	0.00	0.01	0.01	0.01
repeat	99.91	0.00	0.01	0.01	0.01	0.02	0.03
SC#43 - 3	99.97	0.00	0.01	0.00	0.00	0.01	0.01
repeat	99.94	0.00	0.01	0.00	0.01	0.01	0.02
SC#172-1	99.11	0.05	0.05	0.05	0.12	0.22	0.39
repeat	98.75	0.06	0.08	0.08	0.19	0.30	0.55
repeat	97.96	0.09	0.13	0.15	0.31	0.50	0.85
SC#172-2	99.99	0.00	0.00	0.00	0.00	0.00	0.01
repeat	99.96	0.00	0.01	0.00	0.00	0.01	0.01
SC#172-3	99.60	0.04	0.03	0.02	0.05	0.09	0.16
repeat	99.26	0.05	0.05	0.05	0.11	0.17	0.30

Well	35/2-1	
Sample	TS 28601	
	GAS PHASE	
FRACTION	Wt%	Mole%
N2	0.828	0.476
CO2	0	0
C1	99.143	99.509
C2	0.028	0.015
C3	0	0
ISO-C4	0	0
N-C4	0	0
NEO-C5	0	0
ISO-C5	0	0
N-C5	0	0
C6	0	0
C7	0	0
C8	0	0
C9	0	0
C10+	0	0
Sum	100	100

	GAS PHASE
MEAN MOLE WEIGHT	16.10
GAS GRAVITY	0.555
CRITICAL TEMP (K)	190.4
CRITICAL PRESS (Bara)	46.3
Z-FACTOR @ 1 bara & 15°C	0.998
DENSITY (kg/m^3), 1 bara & 15°C	0.673
VISCOSITY (mPa*s), 1 bara & 15°C	0.011
Z-FACTOR @ 60 bara & 12,5°C	0.876
DENSITY (kg/m^3), @ 60 bara & 12,5°C	46.411
VISCOSITY (mPa*s), @ 60 bara & 12,5°C	0.012

Table 6-6. Summary of the PVT analysis from Well 35/2-1.

The results of the PVT analysis (Figure 6-1) show that the Peon gas discovery holds a very dry gas with 99.5 Mole % of Methane.

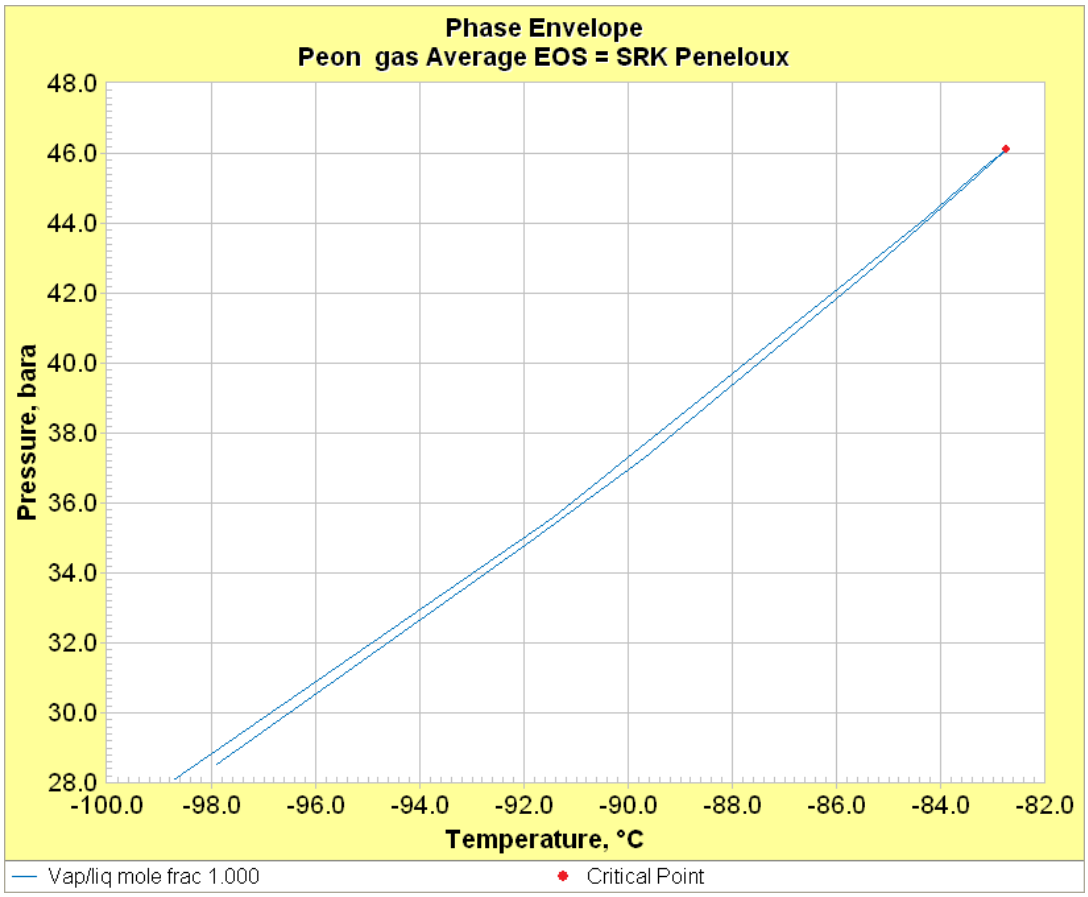

Figure 6-1. PVT analysis shows the phase envelope with the critical point at 46 bar and –82.5 °C

A summary of the molecular composition is given in Table 6-7.

Table 6-7. PT Flash at reservoir conditions.

	PT Flash at 60bar and 12.5 °C
Mole %	100
Weight%	100
Volume	351.6 cm3/mol
Volume %	100
Density	0.0456 g/cm3
Z Factor	0.8881
Molecular Weight	16.1
Enthalpy	-677 J/mol
Entropy	-35.04 J/mol °C
Heat Capacity (Cp)	43.17 J/mol °C
Heat Capacity (Cv)	27.51 J/mol °C

Kappa (Cp/Cv)	1.569
JT Coefficient	0.4343 °C/bara
Velocity of Sound	430.6 m/s
Viscosity	0.0122 cP
Thermal Conductivity	38.87 mW/m °C

6.4 Petrophysical evaluation methodology and results

The petrophysical evaluation of well 35/2-1 is described in this chapter. The interpretation is based on the available logs, fluid tests and samples.

No cores were cut from this well and the MRCT runs (sidewall cores) failed completely.

The resulting CPI is presented in Figure 6.2.

6.4.1 Petrophysical Input Parameters

The petrophysical input parameters used for well 35/2-1are given in Table 4.4-1. Since there is no core data available in this well, the same set of parameters have been used throughout the reservoir.

Table 6-8. Petrophysical Input Parameters

Input parameters well 35/2-1				
Zones			**Peon / Naust**	**Cap rock**
Calculation	**Parameter**	**unit**	**Parameter value**	
V_{sh}	GR_{min} GR_{max}	GAPI GAPI	60 90	75 90
Net sand	**Vsh < 0.5 and Phie > 0.15, Sw < 0.65**			
Log porosity	ρ_{ma} $\rho_{mud\ filtrate}$ $\rho_{HC,\ app}$ ρ_{shale}	g/cc g/cc g/cc g/cc	2.65 1.15 -0.05 2.3	2.65 1.15 1.0 2.3
Archie	a m n R_t R_{xo} R_w @ 15.6 °C R_{mf} @ 20.6 °C Temp @ 582mMD	 ohm-m ohm-m ohm-m ohm-m °C	0.62 2.15 2.00 Deep laterolog (RT_HRLA) PEX/MCFL – RX08 0.0260 0.085 13	0.62 2.15 2.00 Deep laterolog (RT_HRLA) PEX/MCFL – RX08 0.0260 0.0850 13

6.4.2 Net Sand/Shale Volume

The net sand intervals were determined by applying a shale volume cut off of 0.50 and porosity cut off of 15 %.

The shale volume has been calculated from a non-linear relationship with the gamma ray. The reservoir interval is primarily a straightforward sand-shale sequence. The relative abundance of sand and shale is well defined from the gamma ray log, using GFCT factor of 0.5.

The Net Sand definition is insensitive to the porosity cut off, as the Peon reservoir is at much higher porosity than a most likely cut off value. (No cores available.)

6.4.3 Porosity and Permeability

The effective porosity has been calculated from the density log. A linear relationship has been developed. The effective porosity is corrected for shale volume. A HC correction has also been performed, using the Material Balance equation.

(The version called Material Balance method was introduced directly by Hydro, firstly for use in the Troll project. This option uses the form of the density prorosity equation given in this formula: $Sh^*(Dens_{w,a}-Dens_{h,a})$. This gives a more efficient iteration between Porosity (Ø) and Water Saturation (Sw).)

There is some uncertainty in the porosity computation due to the gas correction of the density log. This uncertainty is propagated to the water saturation. However, the uncertainty is not regarded as large, but would have been reduced if core data had been available.

The Peon reservoir properties are very good with an average porosity of 33.2%. In the gas zone the average porosity is 36.0%. Mobilities up to 2700 mD/cP (**Table 6-3)** have been obtained. The other MDT Pressure pre-tests show mobility values varying from 66.5 to 1029.0 mD/cP. The fluid viscosity will be a mixture of gas and mud filtrate, which makes permeability from the pre-tests difficult to interpret.

6.4.4 Water Saturation

The Indonesia equation was used to calculate the water saturation from the logs. The formation water resistivity is estimated based on the MDT water gradient=1.019 g/cc. Schlumberger charts “Resistivity of NaCl Solutions” and “Densities of NaCl Solutions” (Ref. 4.3) have been used as input, obtaining an Rw value of 0.260 ohmm @ 15.6 degC.

Due to the soft formation of Peon, Humbles formula has been used, resulting in the following input parameters: a,m,n= 0.62, 2.15, 2.00.

The formation temperature was collected from the MDT samples. This gave a temperature of 12.8 degC @ 591 meters MD.

Petrophysical input parameters

Table 6-9. Petrophysical zone-averages.

35/2-1	NET SAND INTERVAL				NET PAY	
Zone [m]	Gross [m]	Net [m]	NTG	Porosity [%]	Pay [m]	SW [Frac]
Cap Rock	9.0	0.8	0.085	27.1	0.3	0.443
Peon	33.0	32.6	0.987	33.2	18.4	0.122
Naust	106.0	4.5	0.042	29.2	0.0	-
Total Interval	148.0	37.8	0.255	32.6	18.7	0.127

(*Vsh < 0.5 and Phie > 0.15, Sw < 0.65)*

6.4.5 CPI log

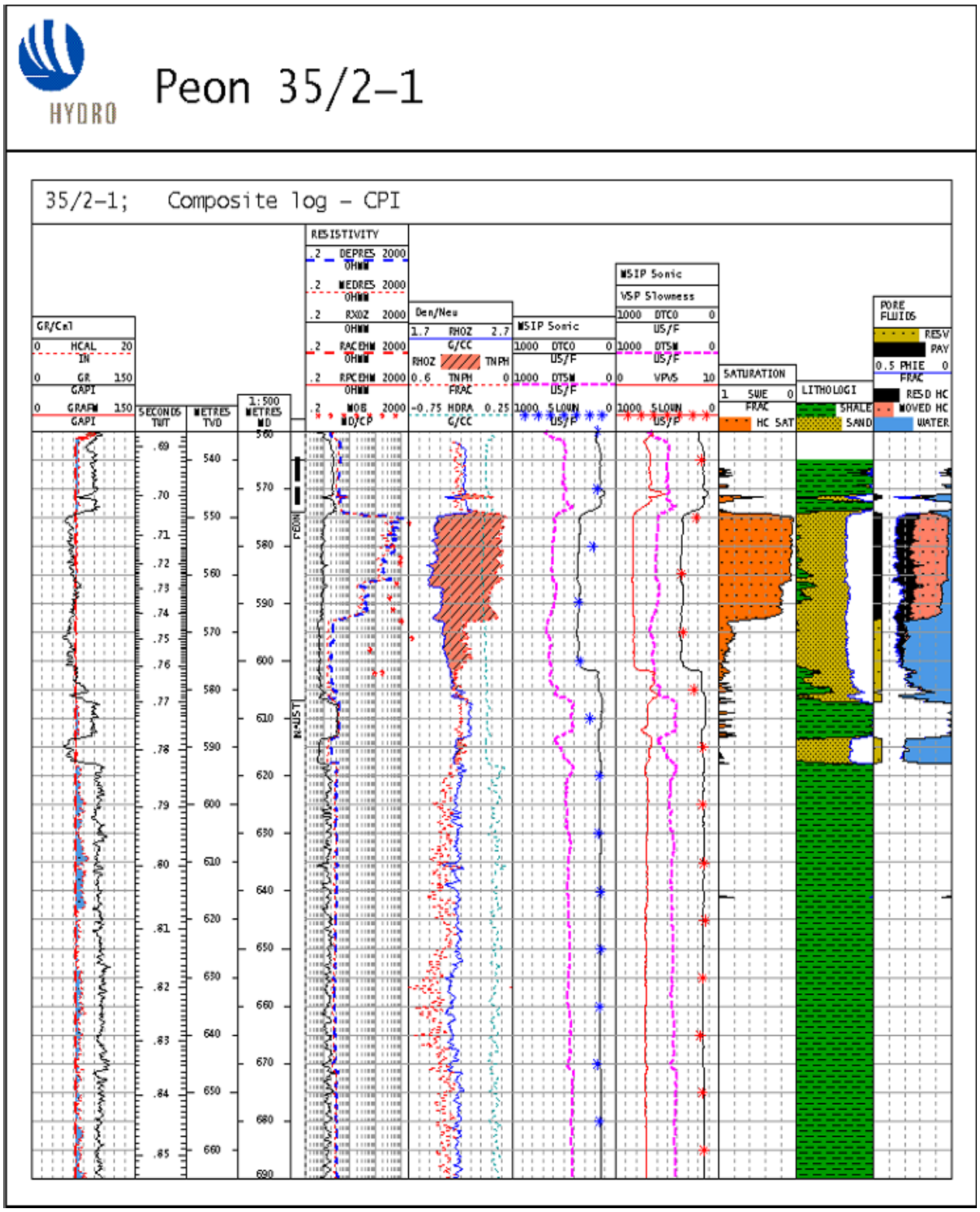

Figure 6-2. Raw logs and CPI.

6.4.6 FMI log

The FMI data were mainly used for interpreting the depositional environment. See Chapter 5.4. FMI Analysis.

6.5 Fluid contact levels

The interpretation of the formation fluid contacts is based on the following information:

Electrical Logs
Formation Pressure Points
PVT analysis (MDT samples)

The data interpreted is discussed below, and a summary of the results are given in **Table 6-10**.

Formation Pressure Points, PVT analysis and Electrical Log Interpretation

The interpreted fluid gradients and contacts are presented in **Figure 6-3**. The gas gradient= 0.046 g/cc is confirmed by PVT analysis of the MDT gas samples. (See **Table 6-6**). The water gradient= 1.019 g/cc is similar to seawater.

The GWC= 593 +/- 1 m MD RKB /568 mTVD MSL is supported by the electrical logs, see **Figure 6-3.** The deep resistivity from the HRLA tool changes dramatically and the CPI shows that there is no longer any movable hydrocarbons below this level.

Table 6-10. Fluid gradients and contact.

Gas Gradient	Water Gradient	GWC
0.046 g/cc / 0.0045 bar/m*	1.019 g/cc / 0.0999 bar/m	593 mMD RKB/ 568 mTVD MSL

: Confirmed by PVT analysis see* **Table 6-6

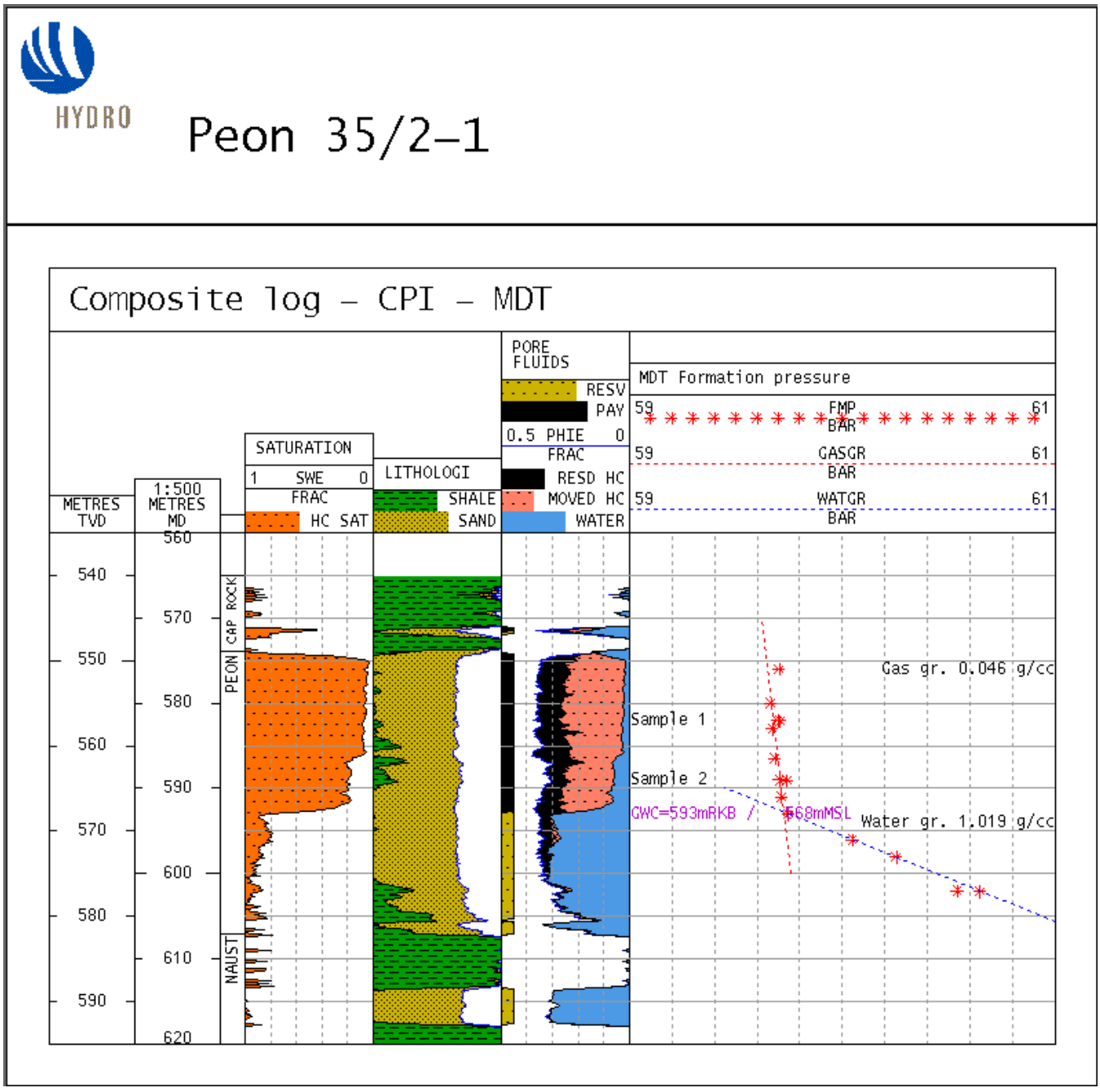

Figure 6-3. Peon Pressure Interpretation

7 HYDROCARBON POTENTIAL

7.1 Base case GOIP estimate

The proven reservoir section in the 35/2-1 well is located within the Pleistocene stratigraphic unit Naust. The glasio-marine mound is interpreted to be a single reservoir, with no compartments due to faults or lithostratigraphic segmentation. The depositional model indicates a lateral thinning towards the edges of the mound. To be able to give a separate set of reservoir parameters to this rim, the BRV has been calculated as two separate units, Peon Main and Peon Rim. The vertical variation within the reservoir unit in the well is assumed to represent the lateral variations within Peon Main unit. Peon Rim is assumed to be a pinch out, hence reduced net - gross parameters.

The Expected volumes in the Peon accumulation are mainly located in PL318. However, a significant volumes is also located in PL269, and minor volumes may extend into the southern block 35/5 (PL294) and to the North in block 6203/10, see **Table 7-1**.

Table 7-1. Peon in place volumes

	P10	P50	Mean	P90
GOIP (GSm3)	31	35.8	36	41.1

It should be noted that only Peon Main unit is penetrated by the well, but the units are interpreted to be in communication.

As illustrated in **Figure 7-1** and **Figure 7-2** the Peon Rim Unit is considered to be a condensed section located as a perimeter surrounding the Peon Main unit. Due to the lack of empiric data from the well regarding this unit, the net gross distribution is defined with a wider range than within the Peon Main unit (**see Figure 7-3**).

The bulk rock volume is calculated based on a top structure map and cut at the GWC as shown in **Figure 7-4**. The Peon Main is interpreted to cover the area of the mound where it is possible to distinguish between top and base anomaly. Within the Peon Rim a 5 m thick isochor is added as a compensation for the tuning effect based on a sensitivity study comparing the amplitude resolution between the full fold 3D, the High Resolution 2D and the PSDM data.

The GOIP-estimate does not include any volume from the cap-rock sand-stringers or the residual zone below the GWC.

Peon Main
The reservoir parameters used to calculate Peon Main is based on the 35/2-1 well results. The vertical variations are interpreted to be representative of the lateral reservoir distribution
See **Figure 7-4** for net gross distribution

Peon Rim
The reservoir parameters used to calculate the Peon Rim volumes have a wider range, due to the lack of empirical data from the 35/2-1 well. The depositional model indicates the condensation of the rim, and this is reflected within the net gross distributions shown in **Figure 7-4**.

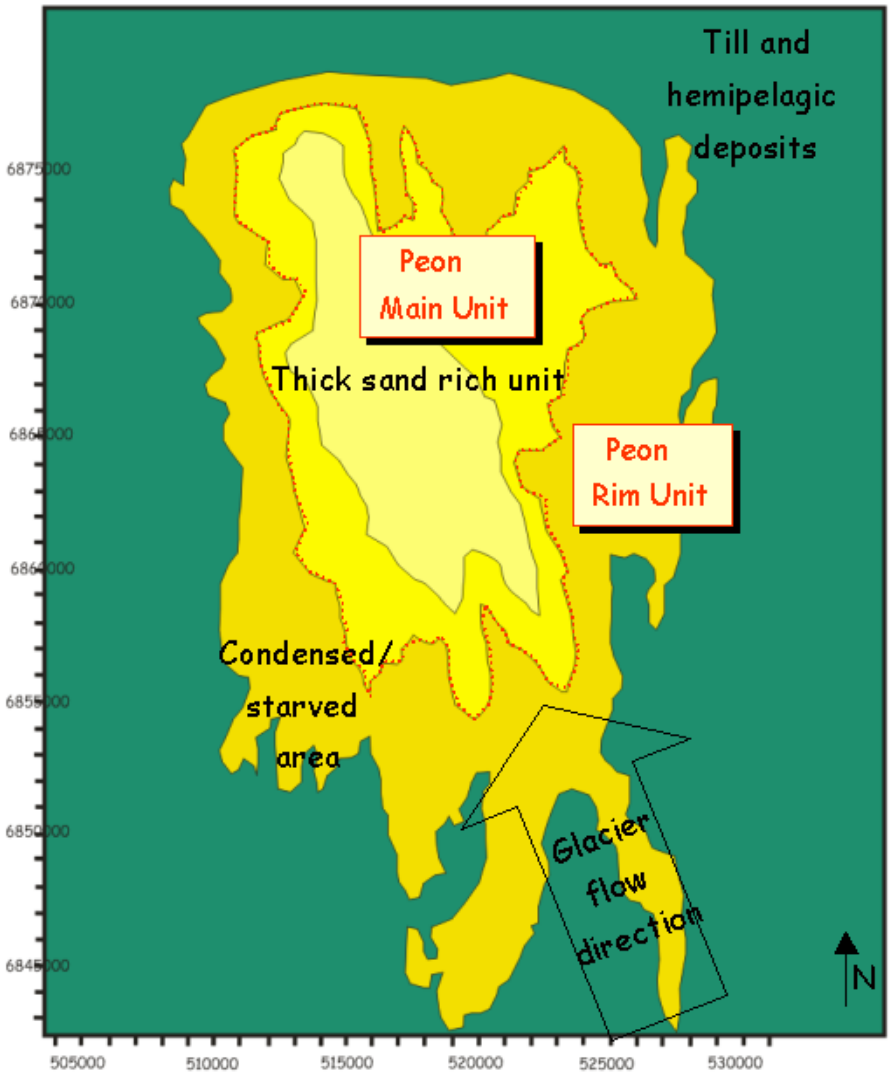

Figure 7-1. Illustrating the lateral distribution of the Peon Main and Peon Rim units.

Figure 7-2. Illustrating the vertical distribution of the Peon Main and Peon Rim units.

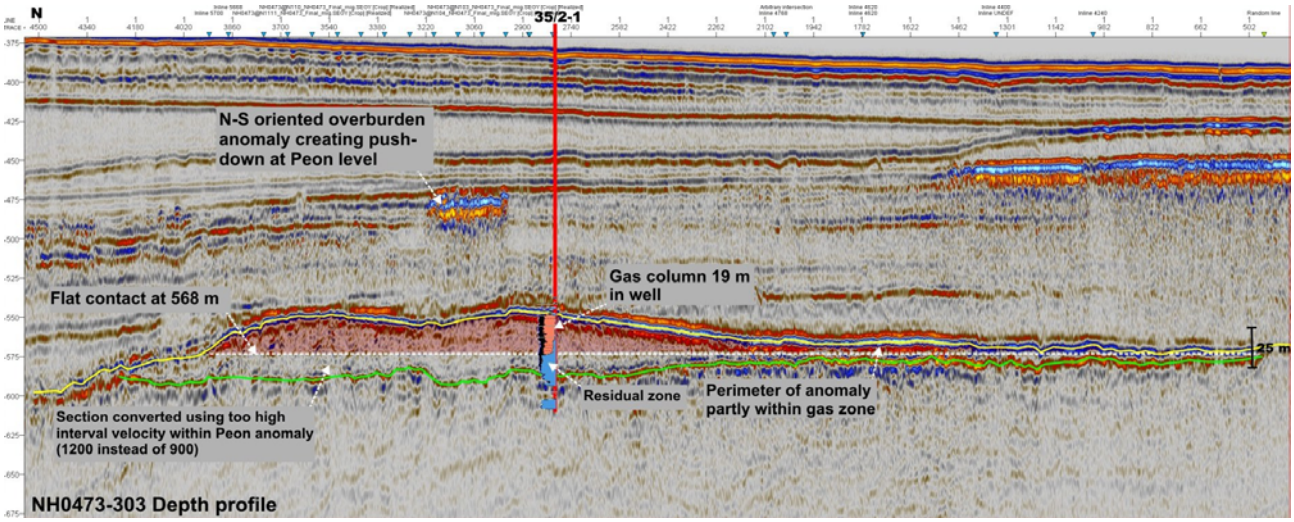

Figure 7-3. The bulk rock volume is calculated based on top structure map, cut on the GWC at 568m MSL. And as a compensation for the tuning effect, the rim is interpreted to be 5 m thick.

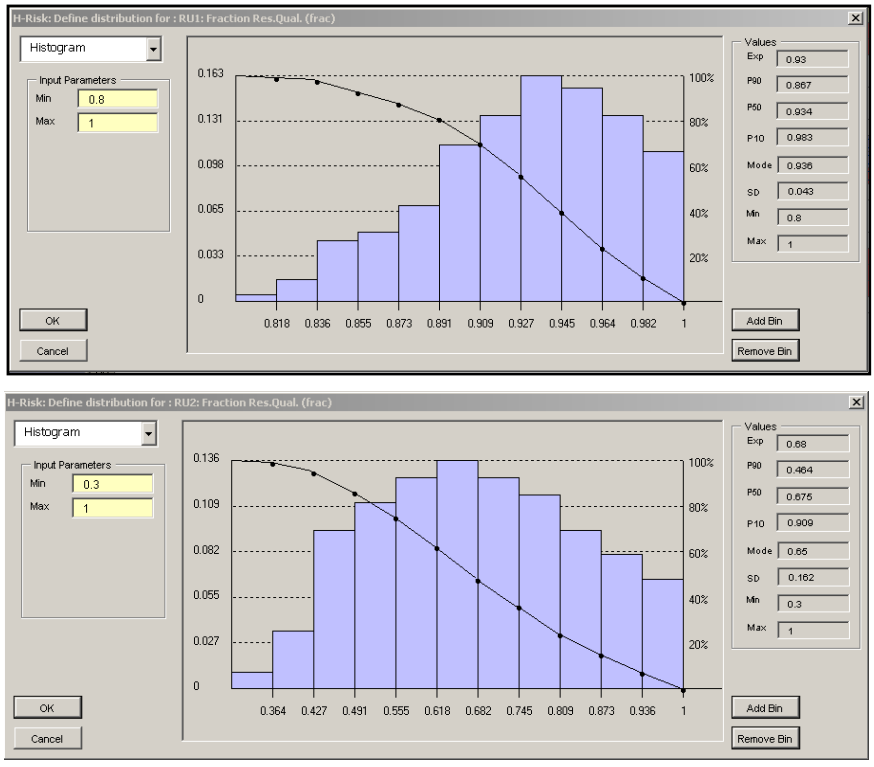

Figure 7-4. Net gross parameter distribution on Peon Main and Peon Rim. Upper panel: Peon Main (fractional reservoir quality). Lower panel: Peon Rim (fractional reservoir quality).

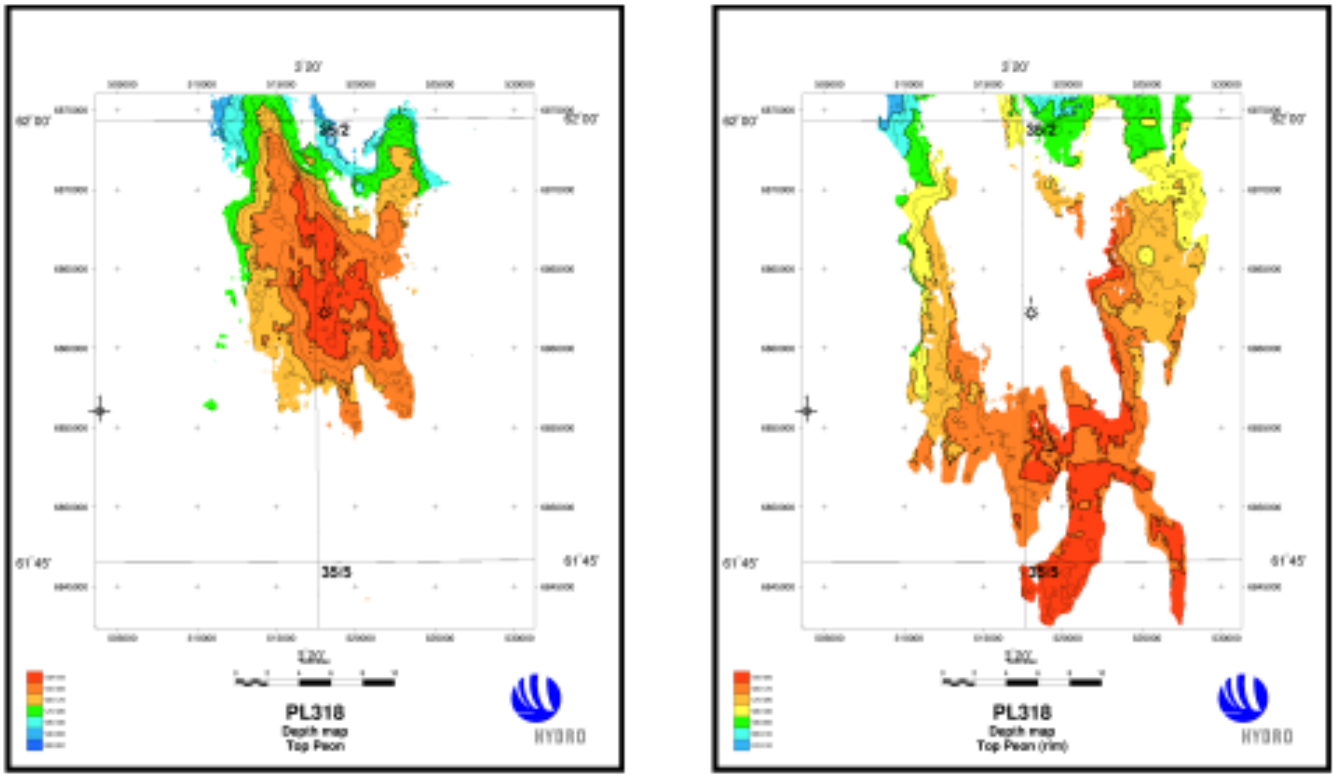

Figure 7-5. Peon Main and Peon Rim structural maps.

The results of the volume calculation shows that the main contributor to the total GOIP is the Peon Main, due to the cut at the GWC, only minor volumes are located within the Peon Rim in the southern part of the structure

Table 7-2. Results from the volumetric calculations of Peon Main and Peon Rim.

GOIP GSm3								
Peon Main			Peon Rim			Total MonteCarlo simulated		
P90	Mean	P10	P90	Mean	P10	P90	Mean	P10
28.7	33.4	38.4	1.0	2.5	4.2	31.0	36	41.1

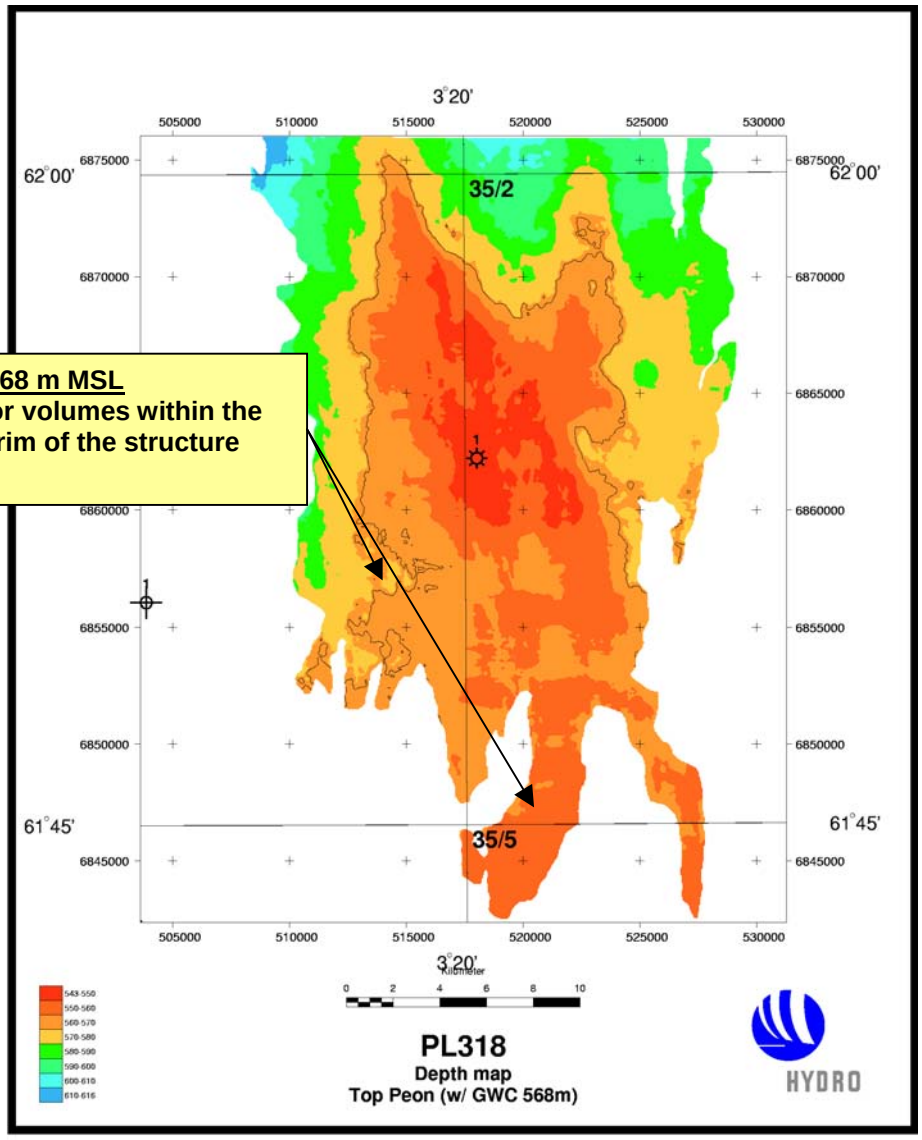

Figure 7-6. Final Peon structural depth map showing the GWC and lateral distribution of the volumes within the mound and perimeter.

8 FIELD DEVELOPMENT CONSIDERATIONS

A technical-economical evaluation has been performed to illustrate potential for economical feasibility of the Peon discovery. A feasible development scenario has been documented as illustrated in **Figure 8-1**:

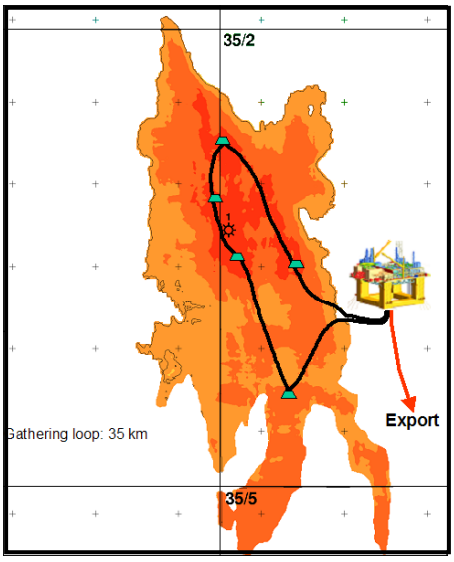

Figure 8-1. Peon field development layout.

This potential development scenario includes 5 vertical production wells that are tied back to a semi-submersible production unit through a field production-loop. The production facility includes processing equipment and living quarters (PQ). The functionality of the processing facility includes mainly power-production, water removal and gas-compression for export.

Export is provided through a 40 km pipeline to the Langeled-North dry gas export pipeline, where hot-tapping is assumed directly into the Langeled-North pipeline.

The Peon field consists of high quality sand with a gas leg and underlying water. Reservoir complexity is expected to be low with good, clean sands and gas composition that is practically pure methane gas. Well productivity is therefore expected to be high, and an average rate of 2 MSm^3/d rate is estimated from each well. Challenges include avoiding water production and ensuring production-well and formation integrity during the depletion process.

The economical analysis indicates that the Peon discovery is sufficiently interesting to initiate feasibility studies. These studies will further mature the reservoir assessment and qualify various development scenarios.

9 REFERENCES

Bugge, T. (1983) Submarine slides on the Norwegian continental margin, with special emphasis on the Storegga area. IKU Publication No. 110.

Gradstein, F. & Bäckström, S. (1996) Cainozoic Biostratigraphy and Paleobathymetry, northern North Sea and Haltenbanken. Norsk Geologisk Tidsskrift 76, 3-32.
Doppert 1980

Haflidason, H., Sejrup, H.P., Bryn, P. and Lien, R. (2001) The Storegga Slide: Chronology and flow mechanism. JOURNAL OF conference Abstracts 6, 740.

King, C. (1989) Cenozoic of the North Sea. In Jenkins, D. G. & Murray, J. W. (Eds.), Stratigraphical Atlas of Fossils Foraminifera, 418-489. Ellis Horwood Ltd., Chichester.

King, E.L., Haflidason, H., Sejrup, H.P. and Løvlie, R. (1998) Glacigenic debris flows on the North Sea Trough Mouth Fan during ice-stream maxima. Marine Geology, 152: 217-246.

NDP Seabed Project (2004) Mid- to Late Cenozoic Geomodel of the Mid-Norwegian Continental Margin. Report no. SP2-02-FS-01R-0001-04

Nilson, S.F. (1996) Sen-Kenozoisk utvikling av nordlige Nordsjø og Nordsjøvifta. Unpubl. Cand. Sci. Thesis, Dep. of Geology, Univ. of Oslo, Norway. 118 pp.

Nygård, A., Sejrup, H. P., Haflidason, H. & Cecchi, M. (2002) 3D Seismic exploration data offshore Western Norway – Evidence of Pleistocene ice streams, subglacial drainage and deglaciation patterns. 32nd Annual Arctic Workshop, March 14-16, 2002. INSTAAR, Univ. of Colorado at Boulder.

Ottesen, D., Dowdeswell, J.A. & Rise, L. (2005) Submarine landforms and the reconstruction of fast-flowing ice streams within a large Quaternary ice sheet: The 2500-km-long Norwegian-Svalbard margin (57°–80°N). Geological Society of America Bulletin: Vol. 117, No. 7, pp. 1033–1050.

Rise, L., Rokoengen, K., Skinner, A.C. and Long, D. (1984) Kvartærgeologisk kart mellom 60°30'N og 62°N, og øst for 1°V 1: 500 000. Institutt for kontinentalsokkelundersøkelser, Trondheim.

Sejrup, H. P., Aarseth, I., Haflidason, H., Løvlie, R., Bratten, Å., Tjøstheim, G., Forsberg, C. F. & Ellingsen, K. L. (1995) Quaternary of the Norwegian Channel; paleoceanography and glaciation history. Norsk Geologisk Tidsskrift 75, 65-87.

Spiegler, D. & Jansen, E. (1989) Planktonic Foraminifer Biostratigraphy of Norwegian Sea Sediments: ODP Leg 104. In Eldholm, O., Thiede, J., Tayler, E., et al. (Eds.), Proceedings of the Ocean Drilling Program, Scientific Results 104: College Station, TX (Ocean Drilling Program), 681-696.

Weaver, P. P. E. & Clement, B. M. (1986). Synchronicity of Pliocene planktonic foraminiferid datums in the North Atlantic. Marine Micropalaeontology 10, 295-307.

Zagwijn, W. H. (1985). An outhline of the Quaternary stratigraphy of the Netherlands. Geologie en Mijnbouw 64, 251-272.

Zagwijn, W. H. (1989). The Netherlands during the Tertiary and the Quaternary: a case history of coastal lowland evolution. Geologie en Mijnbouw 68, 107-120.

APPENDICES

Appendix 1: GEUS (2005) Biostratigrahy and paleoecology of Well 35/2-1. Dinoflagellate cysts and foraminiferal faunes (Report no. 2005/69)

Appendix 2: NPD (2005) Biostratigraphic investigation of Well 35/2-1

Appendix 3: Norsk Hydro (2005) Petrographical analyses, Well 35/2-1 (Norsk Hydro Report no. NH-01189838).

Appendix 4: Eiriksfiord (2005) Geological interpretation from FMI image log, Well 35/2-1 (Norsk Hydro Report no. NH-01159532).

Appendix 5: Norsk Hydro (2005) Well 35/2-1 Petroleum geochemistry (Norsk Hydro Report no. NH-01211349)